EIDGENÖSSISCHE TECHNISCHE HOCHSCHULE LAUSANNE
POLITECNICO FEDERALE DI LOSANNA
SWISS FEDERAL INSTITUTE OF TECHNOLOGY LAUSANNE
FACULTÉ SCIENCES ET TECHNIQUES DE L'INGÉNIEUR
LABORATOIRE DE MICROSYSTÈMES
CH–1015 LAUSANNE

ÉCOLE POLYTECHNIQUE
FÉDÉRALE DE LAUSANNE

Master Project (2007), Microengineering section

The University of Tokyo, Institute of Industrial Science

Development of a Microfluidic Chip Including a Nanochannel for Resistive-Pulse Detection

Mariam Benabderrazik

Professors: Martin Gijs (EPFL), Hiroyuki Fujita (the University of Tokyo)

Assistant: Christophe Yamahata (the University of Tokyo)

February 23, 2007

Development of a fluidic microchip including a nanochannel for the detection and isolation of DNA

This research will be held in the laboratory of Professor Hiroyuki Fujita (University of Tokyo, Institute of Industrial Science). This subject is part of a major project whose final goal is to demonstrate the direct manipulation of a single DNA molecule with a MEMS device.

Section: Microtechnique (diploma project)
Contact: Christophe Yamahata (yamahata@iis.u-tokyo.ac.jp)

Keywords: DNA, Coulter counter, nanofabrication.

We have recently demonstrated the *isolation* and *trapping* of double stranded λ-DNA in a microfluidic chip by means of electrophoresis (EP) and dielectrophoresis (DEP).
The purpose of this project is to develop a fluidic chip combining micro- and nanofluidic structures with integrated electrodes in order to achieve the electrical *detection* of DNA translocation (Coulter counter principle). Such device will eventually be combined with our existing microfluidic system.

Depending on the advance in the project, the student will focus on one of the following milestones (non-exhaustive list):

- Comparison between electrical signal and fluorescence imaging;
- Closed-loop control of EP and DEP with LabVIEW in order to guarantee the translocation of a unique DNA molecule;
- Experiments combining DNA with fluorescence-dyed RNA or protein.

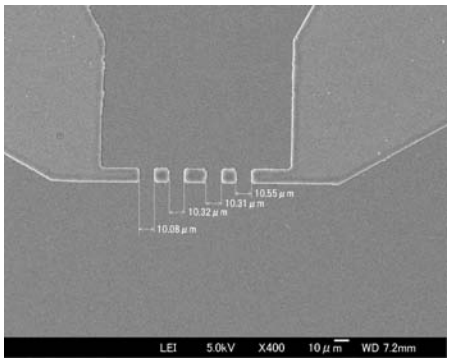

Platinum electrodes on a glass substrate.

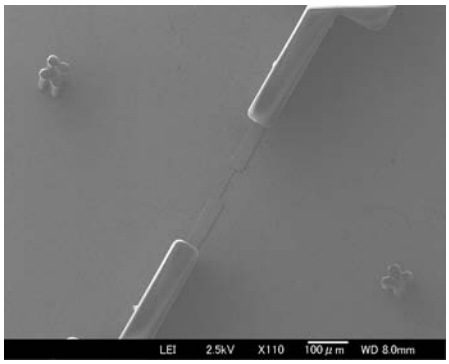

Silicon / SU-8 mould used for the fabrication of micro- and nanofluidic structures in PDMS

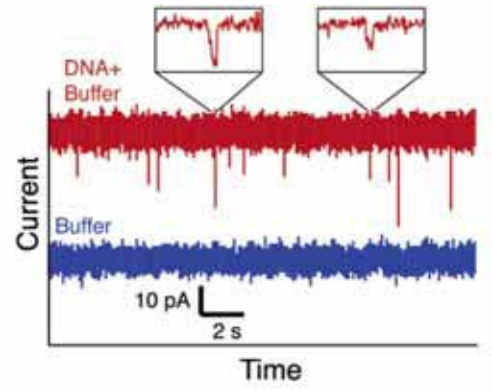

Typical expected measurements.

Ref.: O. A. Saleh and L. L. Sohn, "An Artificial Nanopore for Molecular Sensing," *Nano Letters* ***3***, 37-38 (2003). DOI: 10.1021/nl0255202

Development of a Microfluidic Chip Including a Nanochannel for Resistive Pulse Detection

Mariam Benabderrazik, Microengineering

Assistant: *Christophe Yamahata (Institute of Industrial Science, University of Tokyo, Japan)*

Professors: *Martin Gijs (EPFL); Hiroyuki Fujita (University of Tokyo)*

Motivation

Kumemura *et al.* have demonstrated the isolation and trapping of a single double stranded DNA molecule in a microfluidic chip [1]. However, the detection of DNA molecule was achieved by fluorescent imaging. The purpose of this project was to develop a microfluidic chip capable of performing this detection electrically in order to further automate and enhance the reproducibility of these experiments.

Working principle and fabrication

The resistive-pulse detection method (Coulter counter principle) has been implemented in a miniaturized fluidic device (Fig. 1). The polydimethylsiloxane (PDMS) layer, containing a nanochannel (down to 200 × 200 nm^2 cross-section) and large microstructures, was obtained by moulding. The master was fabricated by electron-beam direct writing (nanostructures) and SU-8 photolithography (high aspect ratio microstructures).

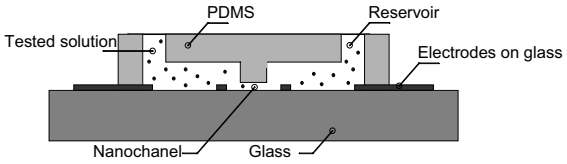

Figure 1: *Schematic diagram of the device.*

For the characterization of the system, we have used polystyrene beads of different diameters in combination with nanochannels of various sizes. A constant DC voltage was applied across the nanochannel through integrated platinum electrodes (Fig. 2).

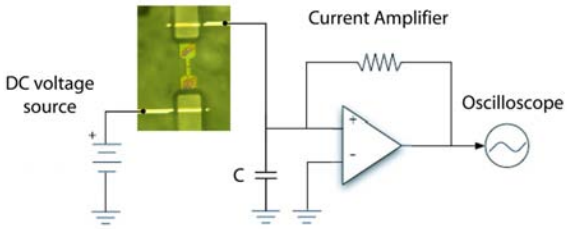

Figure 2: *Resistive-pulse measurements.*

Characterization

When a bead goes through the nanochannel, the resulting change of resistance can be detected with a Current Amplifier. An example of the typical measurements obtained with this setup is illustrated in Fig. 3.

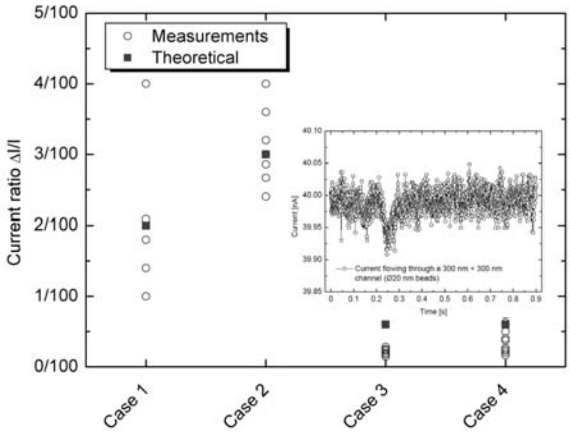

Figure 3*: Measurements of current amplitudes compared with theory.*
Inset: Current pulse of a 20 nm bead in case of a 300 × 300 nm^2 nanochannel (case 3).

[1] Momoko Kumemura *et al*. "Single DNA isolation and trapping in a microfluidic device" (Article submitted), 2007.

Acknowledgements

I would like to express my gratefulness to Professor Hiroyuki Fujita for giving me the opportunity to do my Master thesis in his laboratory. It has been a great honour for me to be a member of the Fujita Laboratory. I also want to deeply thank Professor Martin Gijs for supporting my exchange with the University of Tokyo. I am very grateful to Christophe Yamahata for proposing and supervising this Master project.

Several people have been active in enabling this project to be completed. I would like to thank for the time involved and for their continuous support especially Momoko Kumemura for bio-chemistry, Frédéric Gillot for the processing of the electrodes and Professor Dominique Collard for his precious advices for the electrical measurements. I learnt much and enjoyed working with them. Many thanks to Edin Sarajlic, Ersin Altintas and Tetsuhiko Iizuka for their help on the processes. Thanks also to Professor Omar Saleh for his useful advices on the resistive-pulse detection subject.
I also acknowledge the Institute of Industrial Science for offering me the possibility to attend Japanese classes.

Thanks to Cagatay Tarhan for the shared time during experiments and his support during my stay. I would like to warmly thank all the other members of the Fujita Lab and the members of Fujii Lab with whom I spent appreciated moments. A special thank to Okudaira-san, Ueda-san, Makino-san, Okamatsu-san for helping me with my settlement in Tokyo, and to Naoyoshi Sakaki for helping me with all the Japanese forms filling.

For the unforgettable shared time in Japan, I would like to thank Alcira and Bernard Reymond; Ben and Lukas; Aya, Yu and Kayoko; and all other people I met and with whom I spent enjoyable moments. Finally I would like to thank my parents for their unconditional support, and of course Ips-san.

「ありがとうございました」

Contents

List of Figures

Chapter 1

Introduction

1.1 Context and motivation

The advances in fabrication technologies have opened the path for a new research in fluidics applied to miniaturized biological instrumentation. Indeed, it is believed that micro- and nanofluidic devices have the potential to surpass the performances of standard laboratory equipments either in terms of cost, speed, accuracy or throughput.
In recent years, such devices have been proposed for their ability to isolate, manipulate, and further investigate single biomolecules. To cite a few examples among the techniques developed, one can mention entropic trap arrays, micro- and nanopillar arrays, nanopores or nanochannels [1].

A promising approach for single DNA analysis has been proposed recently by Kumemura[1] *et al.* [2]. They have developed a lab-on-a-chip (LOC) microfluidic device for isolation and trapping of a single double stranded DNA molecule.
To perform single molecule isolation, DNA molecules are driven through microchannels of variable widths by means of electrophoresis (EP), using integrated electrodes. The isolated DNA molecule is then trapped by dielectrophoresis (DEP) with electrodes that are in direct contact with the liquid medium, as shown in Figure 1.1. For these experiments, DNA detection relies on optical fluorescence observation. It is achieved using a fluorescent dye and an inverted microscope. Thus, the activation

[1]University of Tokyo, Institute of Industrial Science

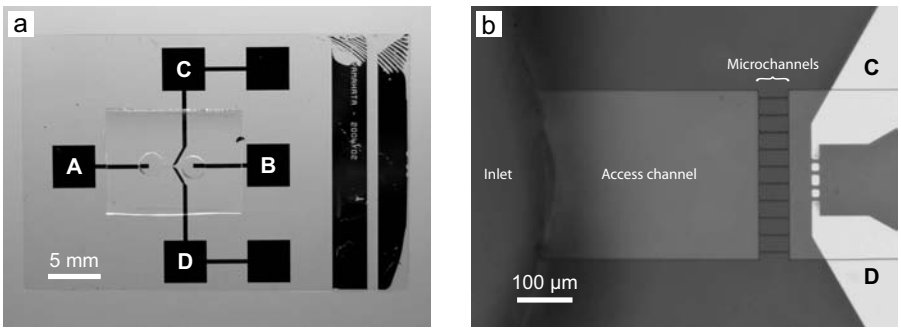

Figure 1.1: A microfluidic device for single DNA isolation and trapping [2].

of DEP when a DNA molecule is nearby the trapping electrodes is done manually, which is a huge disadvantage in regards of time consumption for the manipulations. Indeed, DNA molecules have to be at very low concentration, the size of the molecules combined with the focusing problems due to the molecule's motion and the human reaction time make the manipulation challenging.

Therefore, the purpose of this project is to develop a miniaturized LOC combining micro- and nanofluidic structures with integrated electrodes and using resistive-pulse detection approach (also known as Coulter Counter Principle[2]). In such manner, automated electrical detection and isolation of a single DNA molecule could be performed prior to its trapping.

1.2 Contents

The main body of this report is divided as follows:

- In Chapter 2, we introduce the main **theoretical aspects** and parameters for resistive-pulse detection;
- In Chapter 3, we provide a **state-of-the-art** on resistive-pulse detection method and its applications from micrometer to nanometer scale;
- In Chapter 4, we describe the **design and fabrication** of the microfluidic device;
- In Chapter 5, we present a **characterization** of the device and discuss the results;
- Finally, in Chapter 6, we give a **conclusion** and propose an outlook for this research.

[2]The Coulter counter is a technique that has been developed by W. H. Coulter in 1953 for particle's electrical detection and sizing [3].

Chapter 2

Theoretical Aspects

The main aspects that have to be taken into account for a suitable resistive-pulse detection are:

- **electrical considerations**, including the influence of pore dimension;
- **particle flow** in the fluidic device, which could be performed either electrically (by EP/EOF) or thanks to hydrostatic pressure.

The essential parameters and equations are summarized in this chapter. A comprehensive analysis can be found in the Ph.D. thesis of O. A. Saleh [4].

2.1 Coulter counter principle

W. H. Coulter patented the resistive-pulse detection method in 1953 [3]. As depicted in Figure 2.1, the "Coulter counter" is based on the electrical detection of micron-sized particles passing from one reservoir to another through a small aper-

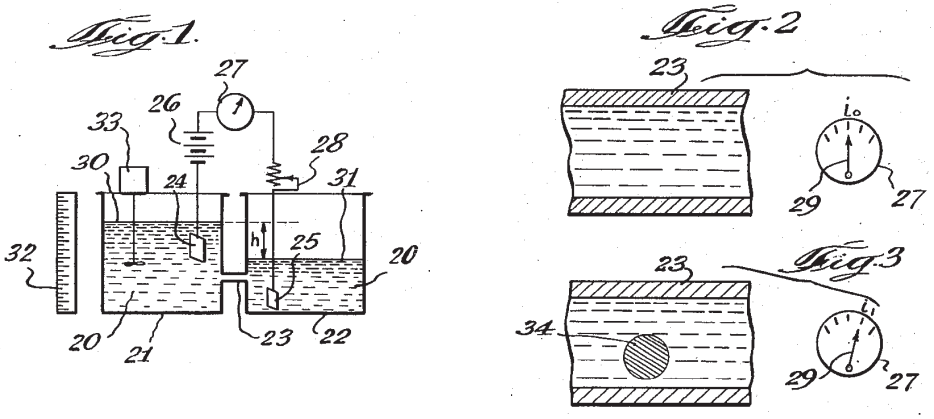

Figure 2.1: Coulter counter principle (US patent 2656508, 1953) [3].(left) Schematic diagram showing the experimental setup; (right/top) The current is measured for a DC potential applied between both sides of the aperture; (right/bottom) When a particle flows through the aperture, a current variation occurs.

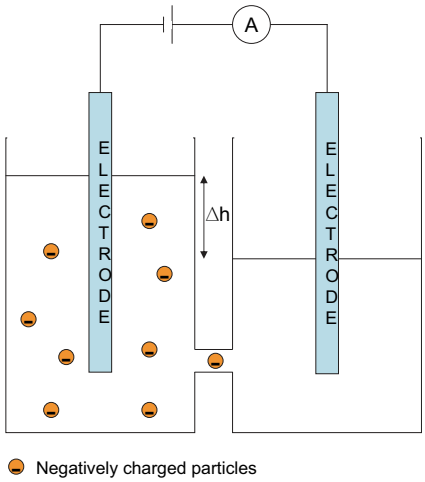

Figure 2.2: Negatively charged particles flow through the Coulter counter.

ture (between 20 µm and 2 mm) by means of hydrostatic pressure.
The reservoirs are both filled with an electrolyte (a conductive solution), and a solution containing particles / biological cells to be sized or counted is introduced in one of them (Figure 2.2). The particles are then driven through the aperture by means of a pressure difference Δh.
By applying a constant DC voltage between two electrodes (one in each reservoir), the impedance can be measured. It remains constant while no particle flows through the aperture (Figure 2.1, right/top). The aperture is dimensioned in such a way that a small variation of its impedance can be detected. Consequently, when a particle goes through the pore (Figure 2.1, right/bottom), it displaces an equivalent volume of electrolyte and modifies the impedance accordingly, providing resistive pulses.
The change of resistance in the aperture depends on the volume of electrolyte displaced. Though, by decreasing the size of the aperture, the device would be sensitive to smaller particles.

2.1.1 Electrical considerations

As seen in Figure 2.1 (right), the aperture in the Coulter counter device can be represented as a variable resistance in an equivalent electrical circuit (Figure 2.3). In order to measure the change in resistance of the pore, two methods are possible according to the Ohmic law ($U = R \times I$):

- By measuring the **voltage variation** across the pore, while the current through it remains constant (Figure 2.3,1a);
- By measuring the **current variation**, while the voltage is kept constant (Figure 2.3,2a).

In the first case, an increase of resistance caused by a particle crossing the pore would increase the voltage (Figure 2.3,1b), whereas it would decrease the current in the second case (Figure 2.3,2b). Both methods can be used. However, as it is

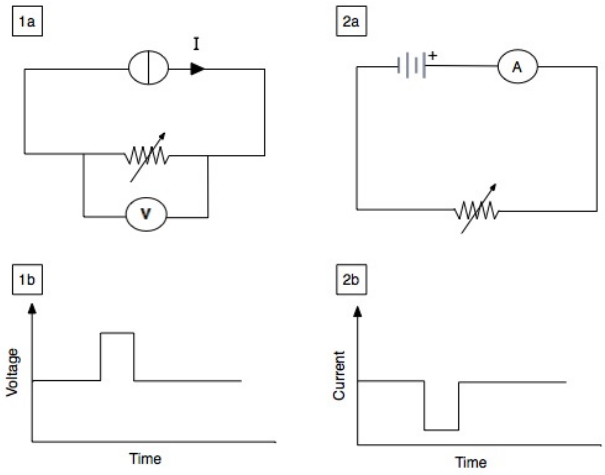

Figure 2.3: Two possible methods for resistive-pulse detection: (1.a) Pore's potential sensing with (1.b) voltage pulse; and (2.a) current sensing with (2.b) current pulse.

usually easier to implement a constant voltage source than a constant current source (depending on the application), the current measurement is preferred in most cases.

Although the equivalent electrical circuit of Figure 2.3 clearly represents the working principle of resistive-pulse detection, it doesn't take into account the behaviour of the electrolyte solution during measurements. In an electrolyte, the application of an electric field across the electrodes leads to the electrode polarization phenomenon, as depicted in Figure 2.4. This led several groups to work on this particular concern and the minimization of its effect [5, 6]. Indeed, the ionic species present in the solution are attracted toward the oppositely charged electrode and form an 'electrical double layer of charge' at the surface of the electrodes.
Due to electrochemical reactions, the ions are either adsorbed or desorbed on the electrodes, even though the polarization ratio diminishes as a function of the electrolyte's concentration (If a lowly concentrated electrolyte is used, the current in the bulk solution between the electrodes will be very low). For this reason, low potential electrochemical reaction electrodes such as silver/silver chloride (Ag/AgCl) are most commonly used in electrophysiology. In our case, the miniaturization of the device

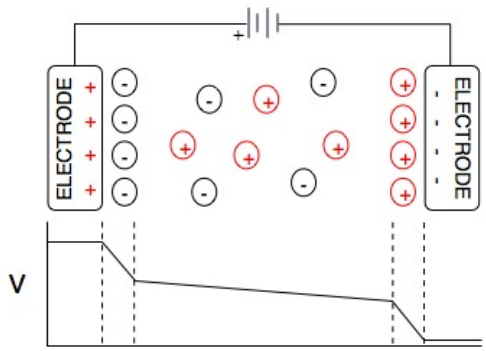

Figure 2.4: Electrodes polarization undergoing electric field [4].

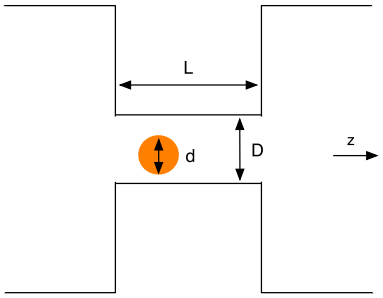

Figure 2.5: Main parameters for the dimensioning of the pore.

implies a miniaturization of the electrodes, resulting in smaller electrodes surfaces. We have chosen platinum (Pt) electrodes because they have a higher electrochemical reaction potential than Ag/AgCl electrodes and can be used with a higher electric field.
The polarisation of the electrodes is an important issue when performing precise measurements, particularly in miniaturised devices.

2.1.2 Pore dimensioning

For resistive-pulse detection, the diameter of the aperture is determined with regards to the size of the particle to be detected because the volume of electrolyte displaced determines the amplitude of pulses.

Signal/Noise ratio On the one hand, *if the pore is too large*, the amplitude of pulses is too low. If it approaches the level of noise, detection becomes impossible to perform. The electrical noise caused by the passage of the ionic current through the aperture is a limiting factor. In the next chapters, we will consider the Noise/Signal (N/S) in order to compare it with the relative resistance or current change.

Pore clogging On the other hand, *if the pore is too small*, the particle's ability to keep in suspension along the aperture is restrained, leading to the obstruction of the pore.

In order to optimize the magnitude of pulses, we have to estimate the change of resistance when a particle crosses the pore. Let's consider a cylindrical pore of diameter D and length L filled with a fluid of conductivity ρ. Its resistance is given by

$$R = \frac{4\rho L}{\pi D^2} \, . \tag{2.1}$$

According to Maxwell and Rayleigh [7, 8], the effective resistance R_{eff} of an infinitely dilute solution of insulating spheres dispersed in a fluid of resistance R is given by

$$R_{eff} = R\left(1 + \frac{3f}{2} + \cdots\right) \, , \tag{2.2}$$

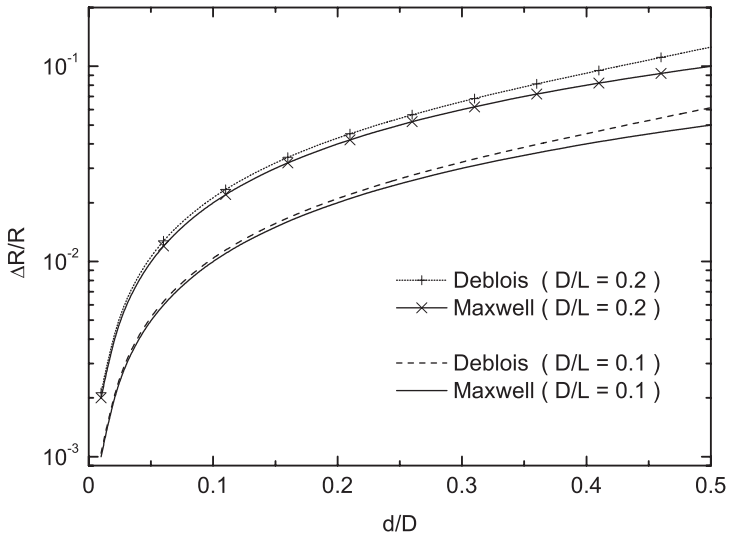

Figure 2.6: Theoretical relative increase of pore resistance as a function of particle diameter to pore diameter ratio (d/D) and pore diameter to pore length ratio (D/L).

where f is the fractional volume occupied by the spheres. When the pore contains a sphere of diameter $d \ll D$ (Figure 2.5), the fractional volume f occupied is

$$f = \frac{2d^3}{3D^2L} \ . \tag{2.3}$$

The expected resistance R' of a pore containing a sphere of diameter d is obtained by substituting equations (2.1) and (2.3) in (2.2):

$$R' = \frac{4\rho L}{\pi D^2}\left(1 + \frac{2d^3}{3D^2L} + \cdots\right) \ . \tag{2.4}$$

The relative increase in resistance, $\frac{\Delta R}{R} = \frac{R'-R}{R}$, is found for the first order of equation (2.4):

$$\frac{\Delta R}{R} = \frac{d^3}{D^2L} \ . \tag{2.5}$$

Maxwell's formulation only applies for infinitely small spheres. Thus, for a wider range of sphere sizes, we can use Deblois and Bean's calculation [9] for the relation:

$$R = \int dR = \rho \int_{-\frac{L}{2}}^{\frac{L}{2}} \frac{1}{A(z)} dz \ , \tag{2.6}$$

where $A(z)$ is the cross sectional area of the empty bulged pore. The increase in resistance upon addition of a sphere to a bulged pore is given by

$$\frac{\Delta R}{R} = \frac{d^3}{D^2L}\left[\frac{D^2}{2L^2} + \frac{1}{\sqrt{1+(D/L)^2}}\right] F(\frac{d^3}{D^3}) \ , \tag{2.7}$$

where $F(\frac{d^3}{D^3})$ is a numerical correction factor given as a table by Deblois and Bean [9]. This factor has been approached experimentally by Saleh [4]:

$$F(x) = 1 + 1.264x + 1.347x^2 + 0.648x^3 + 4.167x^4 \ . \tag{2.8}$$

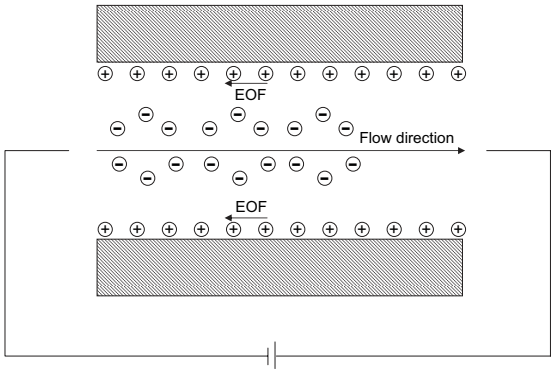

Figure 2.7: Electrophoretic (EP) flow and electroosmotic flow (EOF) induced by an electric potential.

Deblois and Bean's equation is valid only if $d \ll D$, so that the bulge is minimal and the pore can be considered as cylindrical. In that case, the current density is assumed to be uniform all along the pore's cross-section.
In case of large spheres with a diameter close to that of the pore, $d \leq D$, the relative change of resistance is then given by

$$\frac{\Delta R}{R} = \frac{D}{L}\Big[\frac{\arcsin(d/D)}{\sqrt{1-(d/D)^2}} - \frac{d}{D}\Big] \,. \tag{2.9}$$

We can see through equations (2.5) and (2.7) and the plot of Figure 2.6 that the relative variation of resistance in the pore is increased if the diameter ratio d/D is increased and the length of the pore L is decreased. However, to avoid the pore's clogging, we prefer to use a rather low diameter ratio. Also, the length of the pore is limited both by the technology used and the minimum transit time of particles required for detection.

2.2 Electrophoresis versus pressure for particle flow

The particles transit time is a decisive parameter for resistive-pulse detection. Indeed, if the particles pass too fast through the pore, we might not be able to detect the pulse because of the limited sampling frequency of the instrument used for data acquisition. This parameter is directly linked with the particle flow in the microfluidic device. Two methods could be used to perform the particles displacement:

- Electrophoresis (EP),
- Pressure driven flow (PDF).

EP is the migration from negative to positive potential of negatively charged particles under the influence of an electric field (Figure 2.7). Nevertheless, EP also implies an electroosmotic flow (EOF) opposing to the main flow when the electric field is applied through a channel. This is due to a flow of positive charges along the negatively charged surface that drags the surrounding liquid because of viscous

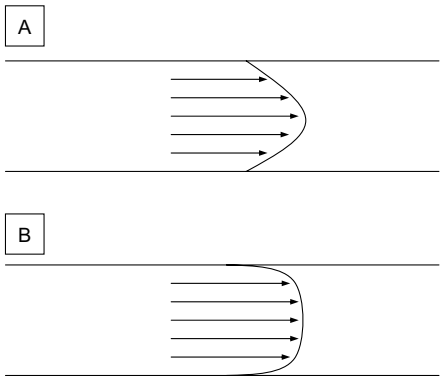

Figure 2.8: (a) Parabolic laminar flow under PDF; and (b) EP profile due to EOF.

forces. The velocity profile is no longer parabolic as it is for pressure driven laminar flow (Figure 2.8).

In the general case, according to Stokes law and considering strictly the forces and velocities in the flow direction, a sphere in a fluid will experience a drag force

$$F_d = -6\pi\mu\frac{d}{2}v_p \ , \tag{2.10}$$

with d the particle diameter, μ the absolute viscosity of the fluid, and v_p the particle velocity. In the pore, a multiplicative adjustment is applied because of the prominent effect of walls:

$$F_d = 6\pi\mu\frac{d}{2}\gamma_1(-v_p + \gamma_2 v_f) \ , \tag{2.11}$$

where $\gamma_{1,2}$ are coefficients for the particle and fluid motion depending on the pore and particle diameter, and v_f is the maximum fluid velocity in the pore.
In case of no fluid flow ($v_f = 0$), for an applied electrophoretic force F_e, the steady state condition leads to $F_e = -F_d$ which, applied to equation (2.11), gives the velocity of a particle undergoing an electrophoretic force:

$$v_p = \frac{F_e}{6\pi\mu\frac{d}{2}\gamma_1} \ , \tag{2.12}$$

The velocity is thus proportional to the applied electric field and inversely proportional to the coefficient γ_1. The relative position of the particle with the z-axis is also a parameter to take into account when performing very precise measurements by means of resistive-pulse [4]. But in the case of particle detection, a variation of up to 10 % is not critical.

The EOF and velocity in a microchannel are influenced by several other parameters listed hereafter [10]:

- In a rectangular microchannel, the flow rate is the lower when height/width ratio tends to 1:1 (square cross-section);
- EOF and velocity decrease when ionic concentration increases;
- Volumetric flow rate and velocity are proportional to the electric field.

EP presents several advantages when compared to PDF. The motion of only charged particles in the liquid prevents from carrying other particles that might clog the pore, and there is less risk of leakage due to pressure in the fluidic channel, though bounding is not necessary. But the most interesting benefit of EP is the precise control of the particle flow and velocity in relation to the applied voltage.

2.3 DNA molecules displacement through a nanochannel

We are not going into detail concerning the DNA structure and properties. However, we can give a brief list of some phenomenons that have to be considered for the experiments with DNA molecules:

- As for all particles in a fluid, Brownian motion occurs, resulting in a small random motion of DNA molecules in the liquid;
- DNA conformations in the channel (see Figure 2.9) would lead to differences in the measured current [1];
- DNA adhesion to the walls when passing through the pore could occur due to the charge of DNA. It could also result in the pore clogging.

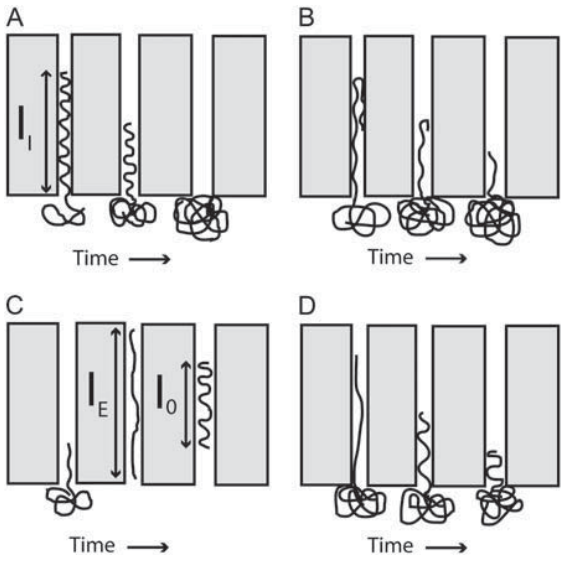

Figure 2.9: Conformation of DNA flowing through a nanochannel [1].

Chapter 3

State-of-the-art

3.1 State-of-the-art on resistive-pulse detection

Many techniques have been developed since W.H. Coulter invented the method of resistive-pulse detection in 1953. The "Coulter counter" is now commercialised by Beckman Coulter CA [11] as an instrument for counting and sizing of biological cells and small particles.
In recent years, single molecule manipulation has brought to the investigation of several essential biophysical phenomenons such as DNA conformation, chromatin organisation or biomolecules interaction dynamics [2]. As a consequence, the possibility of single molecule detection with resistive-pulse detection devices has stimulated the development of new technologies to miniaturize the pores of such systems. A brief summary of the techniques developed so far is given in Figure 3.1.

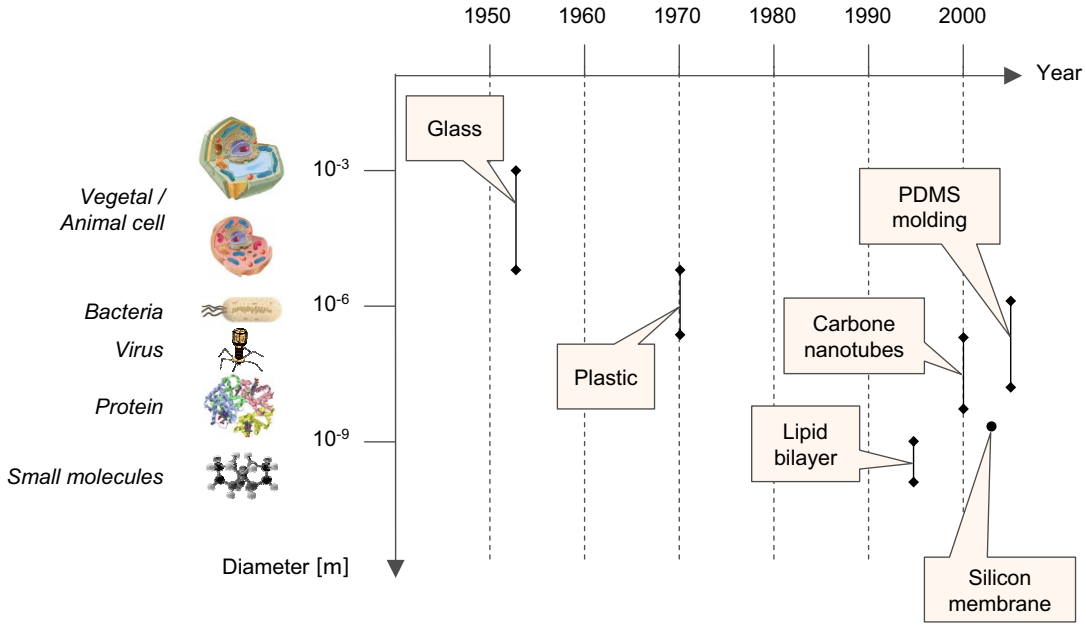

Figure 3.1: Evolution of the use of resistive-pulse sensing in biology since its invention by W. H. Coulter in 1953.

The dimension scale provides a view to their possible field of application in biology. We can distinguish two main categories used for resistive-pulse detection:

- artificial nanopores and natural ion channels in **membranes** (section 3.2);
- integrated **nanochannels** in LOC devices (section 3.3).

3.2 DNA electrical detection using nanopores in membranes

Plastic sheet irradiation with high-energy nuclear particles was achieved in 1970 by Deblois and Bean [9]. They could perform the fabrication of pores from 0.5 µm to 3 µm diameter, thereby enabling colloidal particles (up to 100 nm) sizing and viral particles (∼60 nm) detection with very high precision.
In 1994, Bezrukov *et al.* [12] achieved a striking jump using ion channels in biological lipid bilayer as a pore. This principle is depicted in Figure 3.2. By decreasing the diameter to the nanometre scale, this technique not only allowed for single molecules detection, but also provided the possibility for chemical interaction between the molecule and the pore due to the functional chemical groups in the ion channel's interior walls. Thus, it could probably also be employed as a biosensor.
However, the limited stability of lipid bilayers has led to search for new techniques to fabricate stable solid-state nanopores. Thus, Sun *et al.* have used carbon nanotubes as templates for pores in metallic films [13]. They could achieve 150 nm to 10 nm

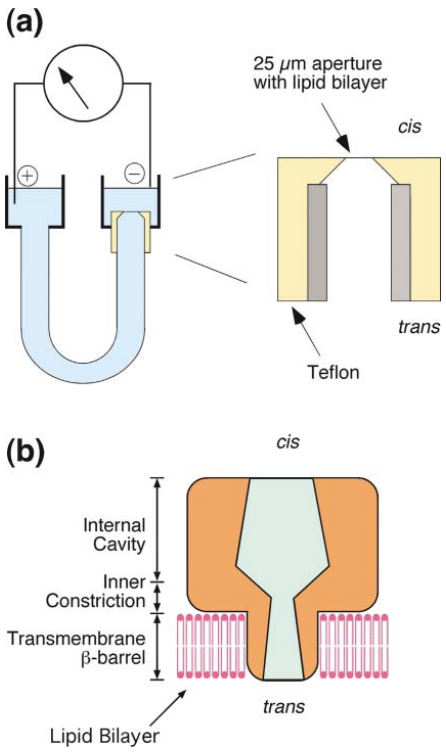

Figure 3.2: An example of a biological channel [14].

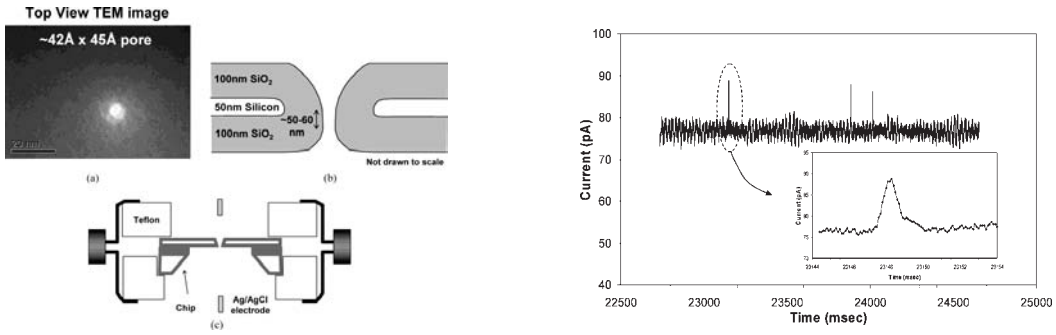

Figure 3.3: An example of a solid-state nanopore in silicon [16].

diameter pores.
Using an ion beam combined with a redeposition method, Li *et al.* have fabricated a 1.8 nm hole in a silicon nitride membrane, as reproduced in Figure 3.3 [15]. Although this method is not as robust as the previous one, DNA molecules (500 base pairs length) sensing could be achieved by this mean.
More recently, single stranded phage DNA (7250 base pairs) and double stranded phage plasmid DNA (6600 base pairs) were sensed using conical nanopores in a track-etched polycarbonate membrane [17]. Scanning Electron Microscope images of such conical nanopores are shown in Figure 3.4: The typical dimension obtained was 40 nm for the tip and 1.5 µm for the base opening.

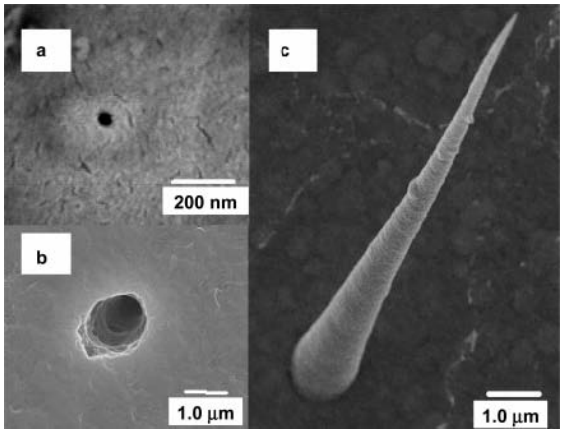

Figure 3.4: An example of a conical nanopore proposed by Harrell *et al.* [17].

3.3 Towards Lab on a chip devices

At the present time, a major task in biological instrumentation is targeted to the development of techniques that are at the same time low-cost and capable of faster automated analysis. Thus, integrating all analysis steps in a miniaturized LOC system seems to be a promising approach. Although the technologies mentioned above have provided good results, they are not compatible with LOC integration and require a complex setup for assembly with fluidic elements.

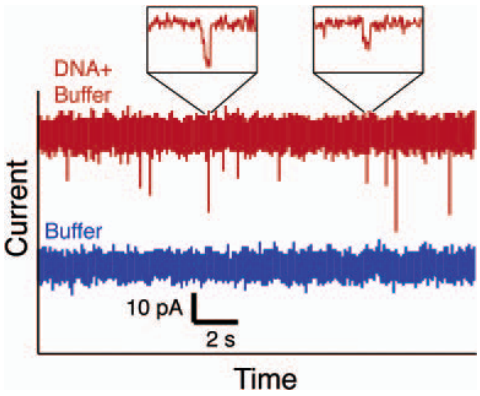

Figure 3.5: Typical current responses for buffer solutions with and without DNA flowing through a PDMS nanochannel [20].

O. A. Saleh and L. L. Sohn have recently developed polydimethylsiloxane (PDMS) microfabricated devices containing pores whose diameters were between 200 nm and 1 µm [18, 19]. Both optical and electron beam lithographies were used to pattern the structures used as masters for PDMS moulding. With such method, they successfully demonstrated the possibility for DNA sensing with a 200 nm × 200 nm nanochannel, as shown in Figure 3.5.
Later on, A. Carbonaro and L. L. Sohn developed multiple pores integrated together on a single chip [21]. These pores were used to detect dimension changes of latex colloids upon specific antigen/antibody binding on the colloid surface.

In our device, the final objective is to perform resistive-pulse detection of a single DNA molecule in a microfluidic chip that could be further integrated in a more complex LOC device. Hence, as we have seen hereinbefore, PDMS moulding would be a more suitable technique than using a pore in a membrane. The device developed in this project is mainly inspired by the latest achievements published by L. L. Sohn and co-workers.

Chapter 4

Design and Fabrication

4.1 Design of the device

The principle of our microfluidic chip is depicted in Figure 4.1. The chip is composed of a PDMS layer stacked on a glass substrate. The PDMS mould consists of a nanochannel for particles sensing, microchannels and reservoirs. For current measurements, we use platinum electrodes deposited on a glass substrate.
Two different configurations have been tested:

1. A single channel design with a central channel of:
    - 1 µm × 1 µm cross-section, 10 µm long
    - 300 nm × 300 nm cross-section, 3 µm long
    - 200 nm × 200 nm cross-section, 3 µm long
2. A 4 channels design with a central channel of:
    - 500 nm × 500 nm cross-section, 3 µm long
    - 300 nm × 300 nm cross-section, 3 µm long
    - 200 nm × 200 nm cross-section, 3 µm long

The dimensions have been chosen to facilitate the capillary filling of the fluidic chip and to reduce as much as possible the fluidic electrical resistance between the measuring electrodes and the nanochannel. As we will see in Chapter 5, the 4 channels device has been designed in order to prevent the particles from passing over the electrodes by the use of 2 supplementary channels.

In the next sections, we will detail the fabrication process which is achieved in three main steps:

- Pt/Ti/SiO_2 deposition of the electrodes on a glass substrate (section 4.2);
- Silicon structuring and SU-8 layer deposition for the mould fabrication (section 4.3);
- PDMS moulding and assembly of the device (section 4.4).

More detailed fabrication flow processes are given in Appendix A.

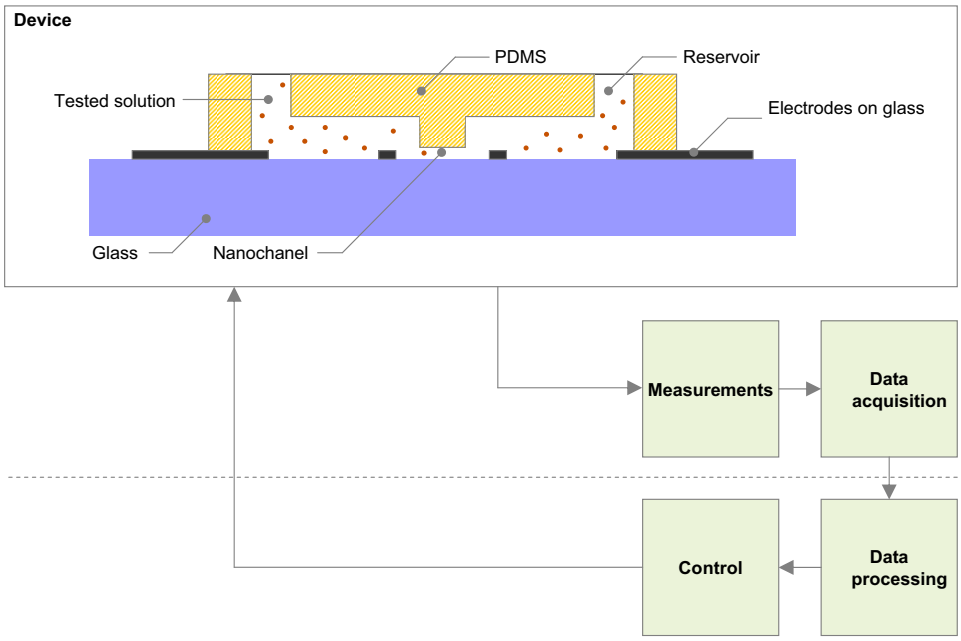

Figure 4.1: Schematic diagram showing the working principle of the device.

4.2 Platinum electrodes on glass

In our miniaturized device, the surface of the electrodes is very small. Therefore, the electrode/fluid interface resistance is increased.

Moreover, the thickness of the electrodes is an important issue for the device's sealing. Thus we use platinum/titanium/Silicon-oxide electrodes ($Pt/Ti/SiO_2$).

The electrodes are deposited on a 24 mm × 36 mm cover glass slide (NEO, Matsunami Glass, Osaka, Japan). The process is described hereafter (the numbers refer to Figure 4.2).

Substrate cleaning

1. The substrate is cleaned using H_2O_2/H_2SO_4 (Sulfuric acid/Peroxide Mixtures, also known as SPM).

Metal sputtering

2. Ti, Pt, and SiO_2 are successively sputtered. This deposition is achieved using a RF Magnetron Sputter (Anelva). In our experiments, the total thickness of the metal layers was around 200 nm. The SiO_2 layer serves as a mask during the etching process, while the Ti layer enables the adhesion of Pt on glass substrate.

Optical lithography

3. HMDS primer (adhesion layer) and S1805 positive photoresist are spin-coated and pre-baked at 60 °C.

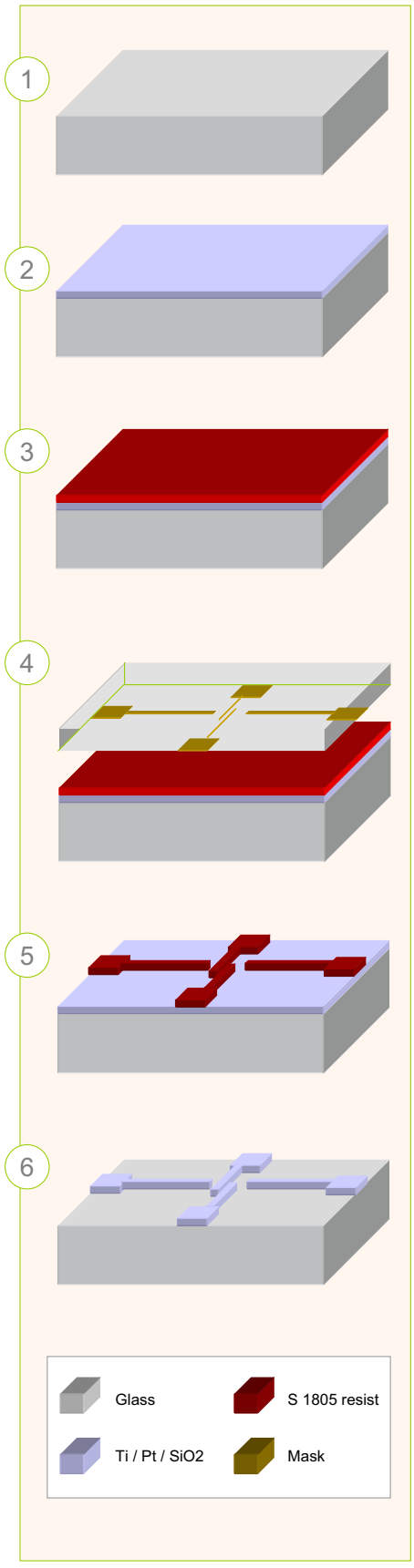

Figure 4.2: Flow process for $Pt/Ti/SiO_2$ electrodes on glass: (1) cleaning, (2) sputtering, (3-5) lithography and (6) etching.

4. The sample is aligned with the mask under a photolithography aligner (Union Aligner machine), it is then exposed to UV light.

5. Development is achieved by means of NMD-3 developer, then we rinse the substrate with deionized (DI) water and post-bake it at 130 °C.

Reactive Ion Etching

6. Reactive Ion Etching (RIE) is performed with a SAMCO RIE-10NR. Only the unprotected deposited metal is etched.

4.3 Mould fabrication

In order to pattern the central nanostructure that will serve as a master for the nanochannel moulding, direct electron-beam (EB) lithography is used, whereas SU-8 lithography is used for the patterning of large microstructures. The wafer used is a standard 300 µm thick, 3" diameter Si wafer.

4.3.1 Electron-beam direct writing

For the electron-beam (EB) writing, the process is illustrated in Figure 4.3. The fabrication steps are as follows:

1. The silicon wafer is cleaned by SPM process.

2. HMDS Primer and the EB resist ZEP 520-A (Zeon) are spin-coated on the wafer.

3. EB direct writing is performed using the 8-inch EB writer F5112+VD01 (Advantest)[1]. Nanostructures of less than 100 nm can be patterned with such equipment.

4. Development is achieved with ZED N50, ZMD-B and Isopropanol (IPA) chemicals. Additional Oxygen Plasma Ashing is performed with the SAMCO-10NR.

5. ICP-RIE is then used for anisotropic etching of silicon utilizing an STS ICP machine (Si etching speed: 1 µm / 15 min). Only the nanostructure, which is protected by the resist, is not etched.

6. ZDMAC chemical and a last RIE etching are used to remove the remaining ZEP 520-A resist.

[1] the direct e-beam writing and the photolitography mask were made at the VLSI Design and Education Center (VDEC, the University of Tokyo).

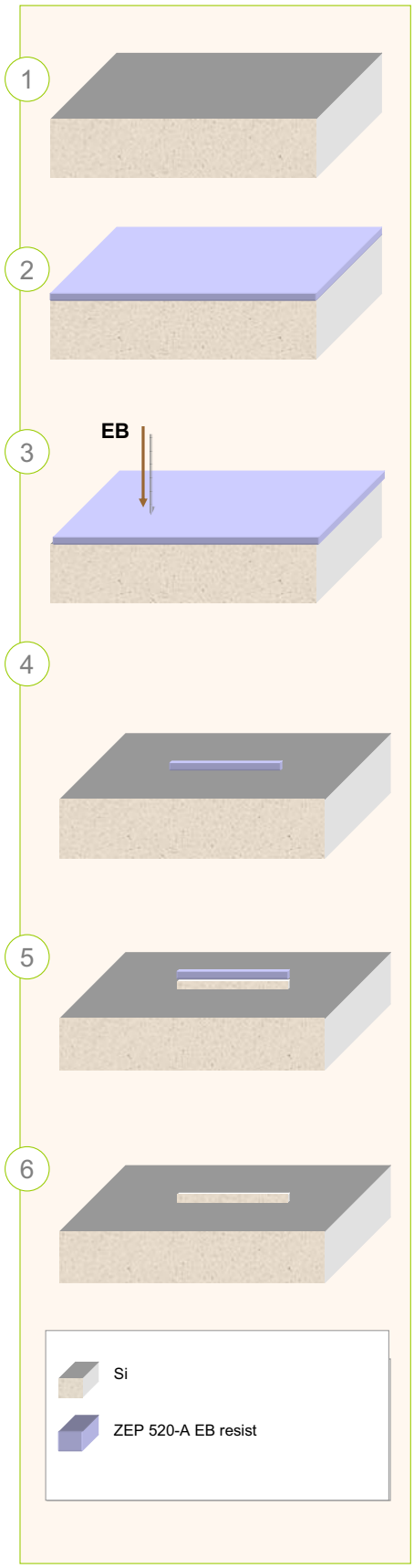

Figure 4.3: Flow process for Electron Beam direct writing of the nanochannel: (1) cleaning, (2) resist spin-coating, (3) EB writing, (4) development, (5) ICP-RIE, (6) resist removal.

4.3.2 SU-8 Lithography

After the EB writing step for nanostructures, we pattern the microstructures in SU-8 thick resist.
The photoresist used is the SU-8 2050 from MicroChem. This high aspect ratio negative resist is suitable for the patterning of ~ 100 µm thick structures. The process flow for this patterning (depicted in Figure 4.4) has been established according to the "SU-8 2000 Processing Guidelines" provided by MicroChem (see Appendix A).

1. The patterned silicon wafer is cleaned by SPM process.
2. SU-8 2050 resist is spin-coated and baked at 65 °C and 95 °C (soft bake).
3. Alignment and exposure are performed using the photography aligner (Union Aligner), and a post-exposure bake is done at 65 °C and 95 °C.
4. The development is achieved in a 'SU-8 developer' bath, two IPA baths and DI water are then used for rinsing. A final hard bake is performed at $150 - 200$ °C for 5 minutes.

4.4 PDMS moulding and assembly

Once Si nanostructures and SU-8 microstructures have been patterned on the silicon wafer, it can be used as a master for PDMS moulding.
The PDMS used is SYLGARD® 184 Silicone Elastomer from Dow Corning (datasheet given in Appendix A). The preparation is performed as described hereafter:

1. The monomer and agent are mixed at 1:10 ratio. In order to make the PDMS surface hydrophilic, we also add to the mixture a droplet (1:200) of a solvent (DK Q8-8011, Dow Corning Toray, Tokyo, Japan), which is a hydrophilizing chemical [2].
2. The PDMS is degassed using a pump until no bubbles are left.
3. A small amount of PDMS is then poured over the structures and spread by tilting the wafer a little in order to have a thin layer covering them.
4. The wafer covered with PDMS is degassed during 5 minutes to make sure that no bubbles could appear in the nanochannel. It is then baked on a hot plate at 100 °C during 5 minutes.
5. The PDMS is then unmoulded carefully and the reservoirs are perforated using a biopsy punch with a diameter of 1.5 mm.

Finally, PDMS alignment with the glass substrate containing the electrodes can be performed using an aligning machine (Union Aligner) by putting the PDMS chip on the wafer support and fixing the glass substrate on a mask. The alignment is then achieved as for usual mask alignments by focusing alternatively on the channels and the electrodes. However, because of the relatively precise alignment needed for our

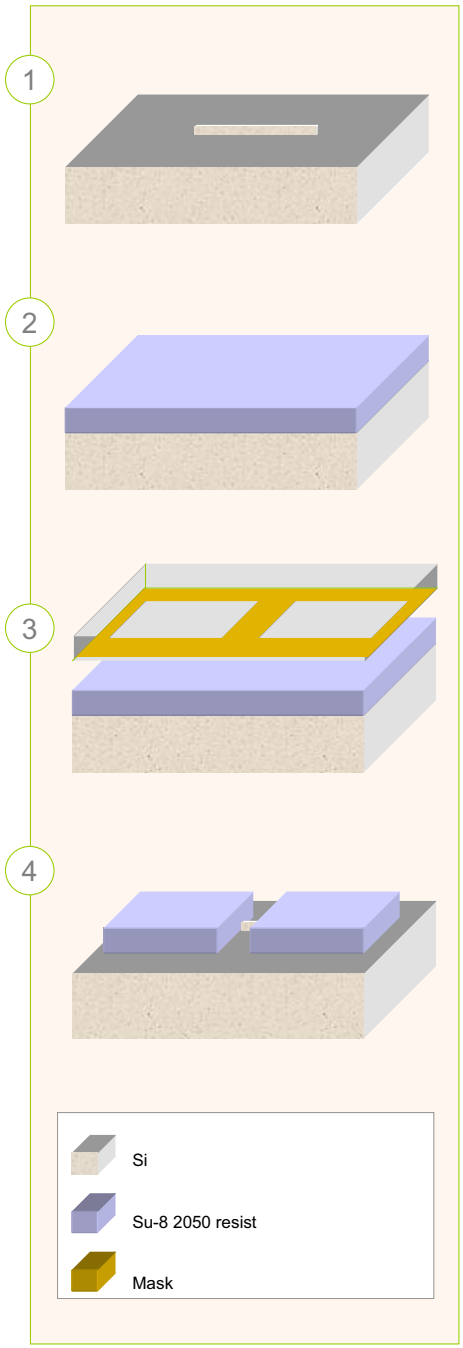

Figure 4.4: Flow process for SU-8 microstructuring: (1) cleaning, (2) resist spin-coating, (3) UV exposure, (4) development.

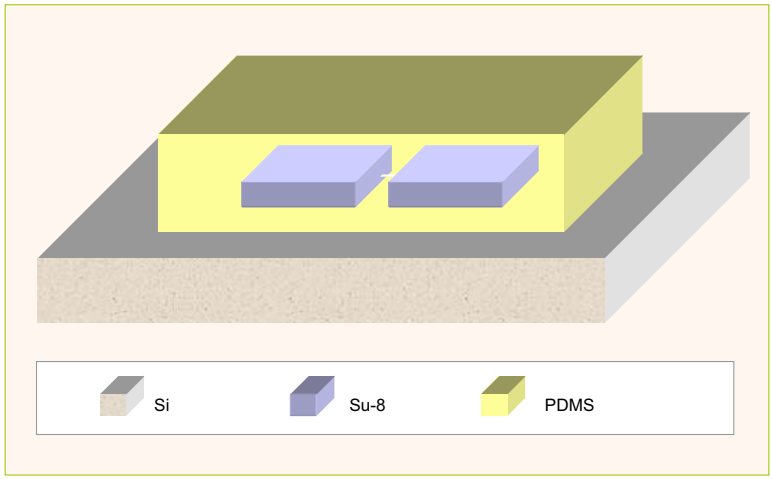

Figure 4.5: PDMS moulding.

design, if the PDMS chip is not perfectly flat, the alignment could become difficult with this method (lost of the alignment during PDMS/glass contact).
Another possibility for the assembly is to use a × 500 optical microscope (i.e. Keyence digital microscope) for manual alignment, as shown in Figure 4.6. By simply pressing slightly on the PDMS, sufficient sealing of the PDMS with glass could be obtained.

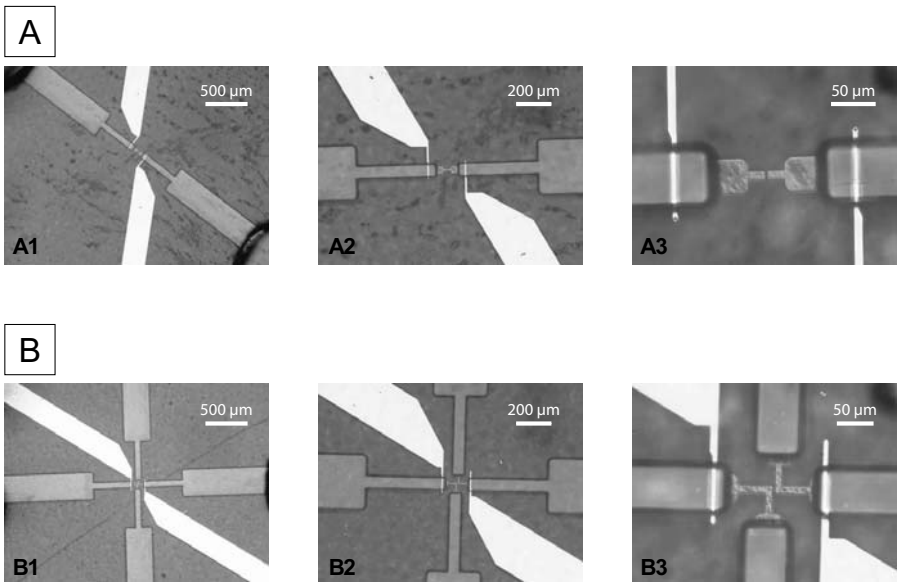

Figure 4.6: Manual alignment of PDMS with electrodes by means of the Keyence microscope. (a) Single and (b) 4 channels configurations.

Chapter 5

Characterization

5.1 Experimental setup

In our design, the resistive-pulse detection is based on current measurement across the nanochannel by applying a DC voltage (Advantest R6240A DC supply) on the measuring electrodes close to the nanochannel, and assessing the current by means of an ammeter (Figure 5.1). Different apparatus allowing two points current measurement were available in the laboratory:

- Patch/Whole Cell Clamp Amplifier CEZ-2400 (Nihon Kohden, Tokyo, Japan)
- Keithley 6487 Picoammeter (Keithley, Cleveland Ohio, USA)
- Keithley 428-P Current Amplifier

However, the Patch Clamp Amplifier is limited in applied voltage at 1.5 V, which restrains the current amplitude. The relatively high N/S ratio inhibited the detection of pulses with lower amplitude ratio. With the picoammeter, the N/S ratio was much lower, but the speed (integration time) is a trade off for its accuracy. The

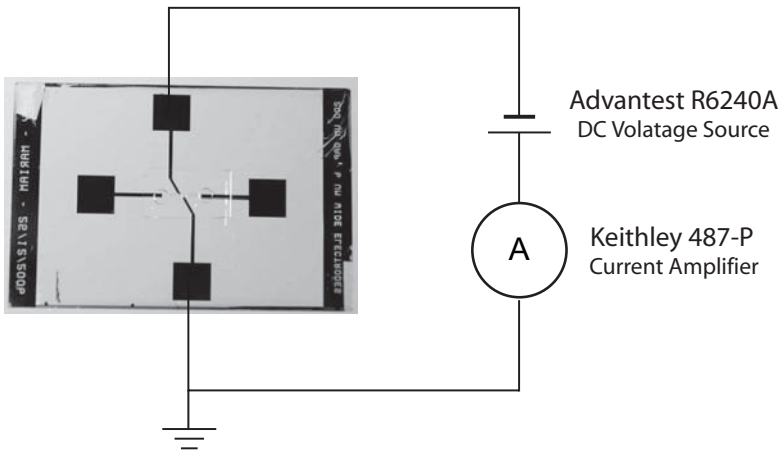

Figure 5.1: Two points current assess across the nanochannel.

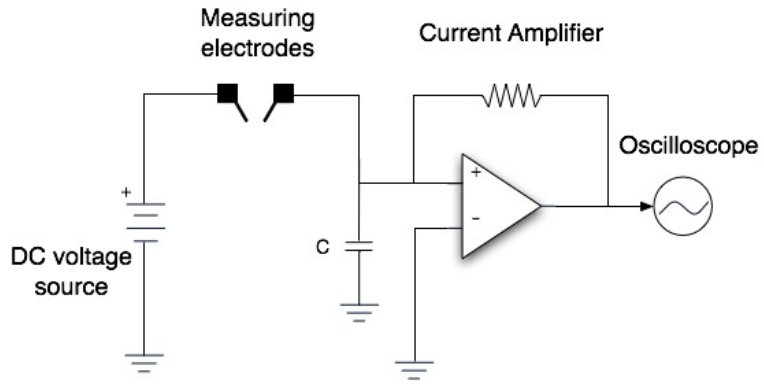

Figure 5.2: Electrical setup for two points current measurement.

pre-amplification settling time on the nA range is in the order of ms, whereas fast acquisition (faster than 1 ms) is a critical requirement for our application.
Therefore, it turned out that the Keithley 428-P Current Amplifier was the most suitable equipment for our measurements. Unlike the picoammeter, the Current Amplifier offers selectable filters to accommodate for noise/speed tolerances. The 10-90% rise time can be configured as fast as 250 µs on the 10^{11} gain range with a 2 pA RMS noise level according to the company's datasheet (see Appendix A). Nevertheless, the current amplifier does not offer an internal Analogic/Digital converter but has a 0–10 V analog output which can be used with a data acquisition board, a real time display or an oscilloscope.

The Keithley 428-P Current Amplifier is connected in series with a R6240A DC Voltage supply (Advantest, Tokyo, Japan). As shown in Figure 5.2, the voltage source is connected to one of the measuring electrodes, while the other electrode is connected to the Current Amplifier, which forces it to the ground. The data are then observed on a Tektronix TDS 2014B Digital Storage Oscilloscope and recorded thanks to a USB key. Because of the very low level of current variations that we wanted to measure, we had to reduce as much as possible the noise. This was achieved with the use of a Faraday cage, coaxial cables and very short connections (Figure 5.3).
Despite all these precautions, a sensitive connection subsists between the electrode and the current amplifier, creating a parasitic capacitance that we had to take into consideration. Moreover, the inverted microscope IX-71 (Olympus, Tokyo, Japan) combined with a Hamamatsu CCD camera (Hamamatsu, Japan) - 300 RCX (Dage MTI, Michigan City, Indiana, USA) and an Image Intensifier (C9016-1, Hamamatsu) unit were used to observe the behaviour of the particles in the microfluidic device by means of fluorescence. The lens used for these observation was an oil immersion lens UPlan Apo ×100 (Olympus, Tokyo, Japan). Unfortunately, as a consequence of the necessity of the Faraday cage, we could not observe and measure simultaneously, which would have been very interesting. However, by connecting the DC voltage source on one of the measuring electrodes, and the other electrode to the ground as we can see in Figure 5.4, the same conditions were reproduced during video recordings.

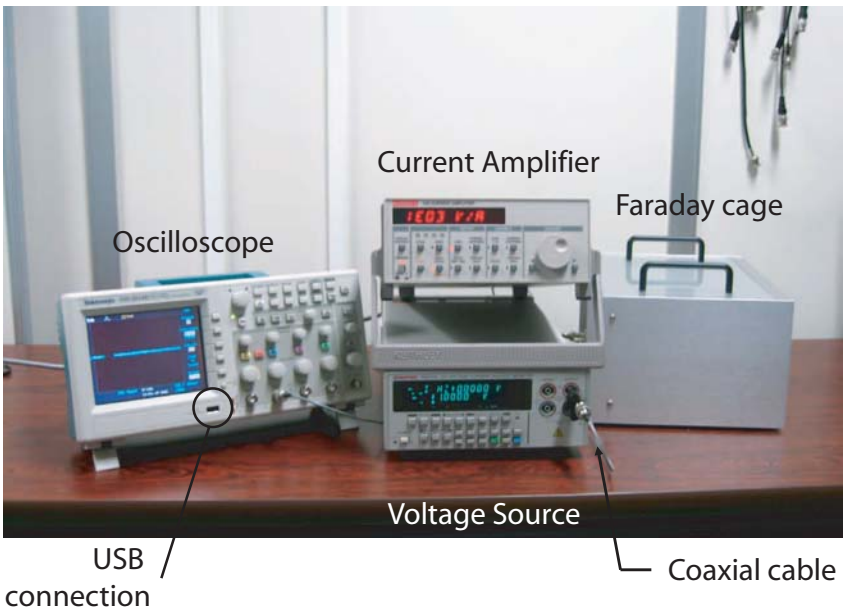

Figure 5.3: Photograph of the electrical setup.

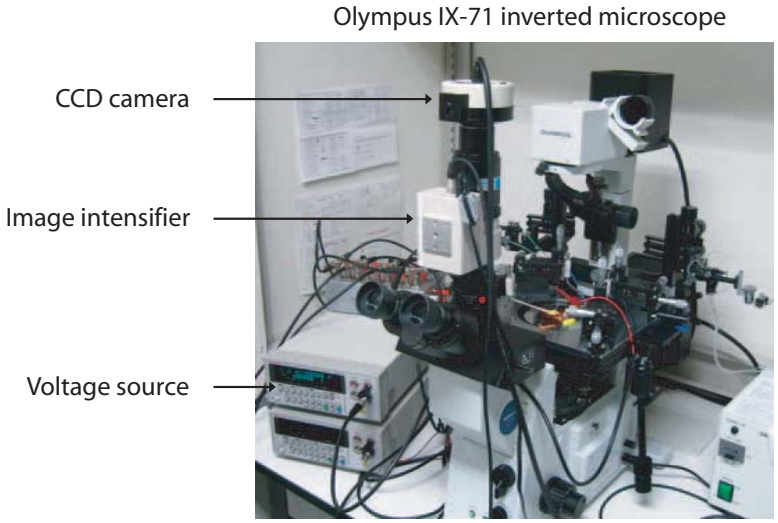

Figure 5.4: Photograph of the optical detection setup.

5.2 Experimental protocol

The experimental protocol can be separated in three main steps:

1. Buffer and particles preparation;

2. Fluidic chip filling;

3. Optical observation and electrical measurements.

5.2.1 Buffer and particles preparation

To characterize our device, fluorescent spheres of different sizes with a diameter ratio in respect to the diameter of the nanochannel (d/D) from 0.2 to 0.066 were used. Table 5.1 summarises the sizes and references of used fluorescent negatively charged spheres for particles sensing. Because of their hydrophobic character, the spheres tend to agglomerate. Consequently some conditions have to be fulfilled according to the products datasheets (Appendix A):

- Low concentration of particles.
- Low concentration of electrolyte.
- Avoid surface charge groups neutralisation.

Hence the suspension containing the spheres is diluted (1:1000) in a 0.1 M KCl solution used as a buffer in order to have a conductive electrolyte and a sufficient concentration of particles to observe high frequency pulses during the measurements.

Beads specifications	**Company**
0.2 µm Sulfate-spheres, 2 % solid	Molecular Probes
0.1 µm Carboxylate YG microspheres, 2 %solid	Fluoresbrite™
0.02 µm Sulfate-spheres, 2 % solid	Molecular Probes

Table 5.1: Fluorescent spheres diameter and provider.

5.2.2 Filling of the microfluidic chip

The buffer solution is introduced from the punched inlets in both sides of the channel and leach into it by capillary force. The liquid run parallel to the microchannel's walls and fills the nanochannel first, then it goes slowly in the microchannels (see Figure 5.5). To reduce the filling time, 5 min vacuum can be used to get the buffer into the microchannels.

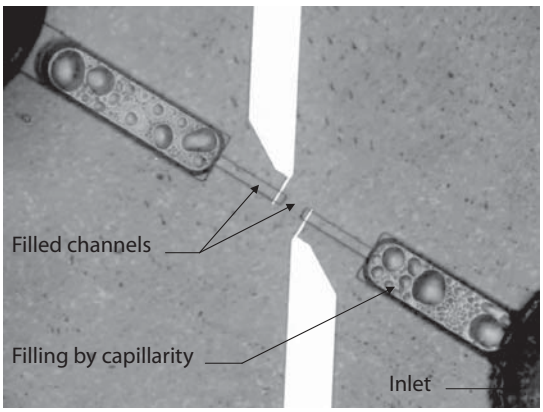

Figure 5.5: Filling of the microfluidic chip by means of capillary force.

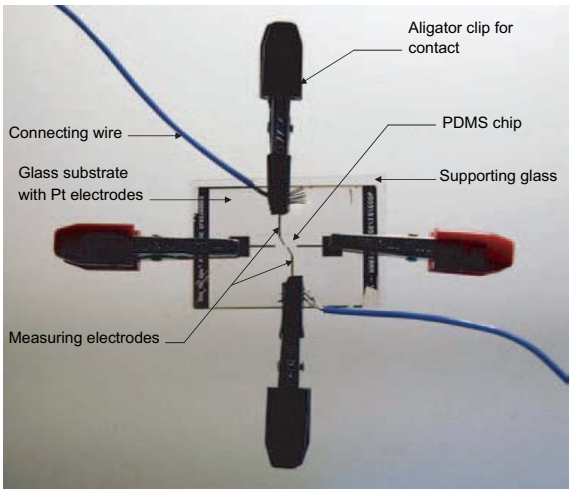

Figure 5.6: Chip prepared for electrical measurements.

5.2.3 Optical observation and current measurements

Once the chip has been filled with the buffer, we use a thicker glass substrate as a support and alligator clips to make the electrical connexions, as shown in the photograph of Figure 5.6. The current across the nanochannel is then measured as described in the electrical setup of Figure 5.1 in order to get a reference signal. The particles to be detected are then introduced in one of the reservoirs and driven by pressure gradient (which is obtained by the height difference in the reservoirs). The use of a syringe pump for pressure was not possible due to the precise alignment inhibiting the use of a bounding between the glass substrate containing the electrodes and the PDMS chip.
The particles in the fluidic chip are then observed by fluorescence using the setup described in section 5.2 in order to check their transit time across the pore under pressure gradient and applied field (Figure 5.7). Once the transit time has been checked, the current measurement can be performed. During the measurements, evaporation occurs. In order to prevent the fluidic chip from drying and to keep the electrolyte concentration constant, the same volume of DI water is added in both reservoirs progressively.

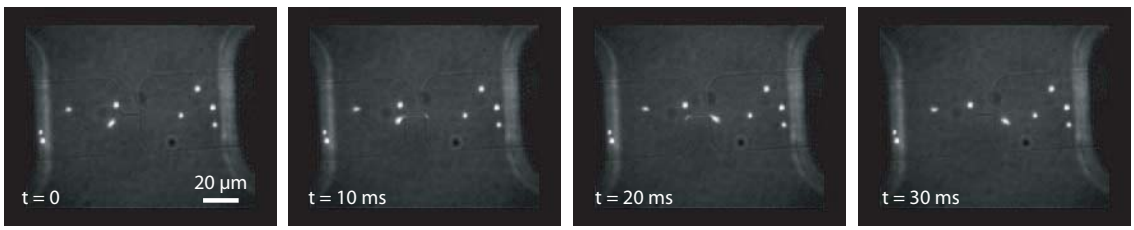

Figure 5.7: Transit time checking by means of fluorescence. Videoframe taken for 200 nm particles flowing through a 1 µm × 1 µm × 10 µm channel.

5.3 Results and discussion

The following aspects have been investigated:

- The most suitable voltage to apply for performing the current measurements;
- The particle flow in the microfluidic device;
- The particles detection characterization;
- DNA detection;

5.3.1 Applied voltage

Table 5.2 shows the measured current output and noise to signal ratio functions of the applied voltage. We can see that the higher the input voltage, the higher the output signal will be. Besides, the amplitude of pulses will also be increased and we will obtain a more favourable noise to signal ratio. However, the applied voltage is limited by the heat power P to dissipate in the nanochannel due to Joule effect, which is proportional to the squared applied voltage U according to the equation $P = \frac{U^2}{R}$, where R is the resistance in the nanochannel. Not only the temperature increase will result in bubble generation and leakage at the nanochannel, but it will also affect the resistance in the nanochannel, thence the measured current. For this reason, we have used a maximum voltage value of 2.5 V in our experiments. The difference between the theoretical and experimental current output is also due to the limited surface of the electrodes and the polarization effect discussed in section 2.1.

Voltage input	**Current output**	**Noise/Signal ratio**	**Theoretical current**	**Theoretical heat power**
1 V	0.2 nA	$\pm 7.5 \times 10^{-2}$	90 nA	0.09 µW
2.5 V	80 nA	$\pm 5 \times 10^{-3}$	227 nA	0.57 µW
5 V	500 nA	$\pm 8 \times 10^{-10}$	454 nA	2.27 µW

Table 5.2: Theoretical current output and heat power versus measured current output and N/S ratio. The reported values are for 0.1 M KCl solution in 1 µm × 1 µm channel.

5.3.2 Particles flow in the microfluidic device

To control electrically the speed of the particles, the first idea was the use of EP by applying a DC voltage on the external electrodes. With such method, we thought that we could control the particles transport across the channel and at the same time perform the current measurement on the internal electrodes. However, because of the measurement setup used in Figure 5.2, this configuration could not be possible. Thus, we have chosen to drive the particles through the device by means of a low-pressure gradient. Indeed, the measuring electrodes in the single channel design Figure 4.6,a) stand for a potential barrier for the negatively charged particles while

performing the current measurement. On the one hand, if a negative potential is applied on the electrode, the particles will tend to move away from it in both directions, resulting in a lack of particles between the measuring electrodes when all the particles located in the sensing area have passed the detection channel. On the other hand, if we apply a positive potential, the particles will tend to agglomerate on the electrode. Consequently we designed the 4 channels fluidic chip (Figure 4.6,b) to avoid the particles crossing over the electrodes.

5.3.3 Particles detection

For the device characterization, we have used the fluorescent spheres listed Table 5.1 in different types of nanochannels. In all the cases presented hereafter, the applied voltage was 2.4 V and the particles were driven through the channel by a low pressure gradient.

- 200 nm diameter particles sensing in 1 µm × 1 µm cross-section, 10 µm long channel in Figure 5.8 (single channel configuration).
- 20 nm diameter particles sensing in 300 nm × 300 nm cross-section, 3 µm long channel in Figure 5.9 (4 channels configuration).
- 20 nm diameter particles sensing in 200 nm × 200 nm cross-section, 3 µm long channel in Figure 5.10 (4 channels configuration).

As we have seen before, the resistive-pulse width is proportional to the current variation:

$$\frac{\Delta R}{R} \propto \frac{\Delta I}{I} \,. \tag{5.1}$$

Thus, comparing the theoretical relative variation of resistance (given by Maxwell and Deblois/Bean, see Chapter 2) with the relative current variations obtained, we can see in the plot of Figure 5.11 that the experimental measurements match well with the theoretical value. We can notice that the use of 300 nm and 200 nm diameter channel (case 3 and 4, respectively) for 20 nm diameter particles is equivalent in terms of the theoretical relative variation of resistance. This is due to the equivalent ratios of d/D and D/L in these cases. The variance between the theoretical and experimental relative current variation could be due to different causes listed hereafter.

- Since we don't have square pulses, we assume that the particle's speed is too high to reach the effective pulse amplitude, which implies a lower relative variation than expected.
- The particle's relative position in the channel's cross-section (relative position to the z-axis). As discussed in section 2.1.1, it is also a parameter that introduces a variance in the pulse's amplitude, especially in our case where we have a small d/D diameter ratio.
- The particles aggregation in some cases leads to bigger elements crossing the nanochannel, thus increasing the pulse amplitude.

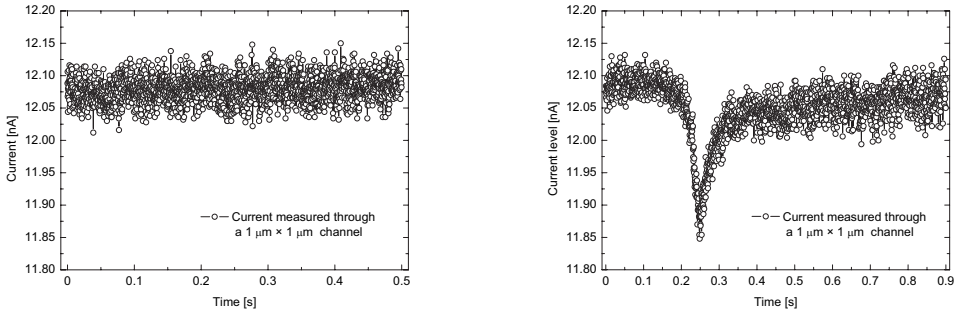

Figure 5.8: Current measurements through a 1 µm × 1 µm cross-section, 10 µm long channel. (a) Buffer solution; (b) Solution containing 200 nm diameter particles.

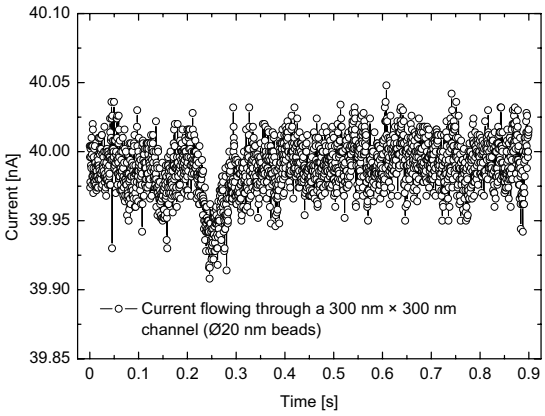

Figure 5.9: 20 nm diameter particles sensing in 300 nm × 300 nm cross-section, 3µm long channel.

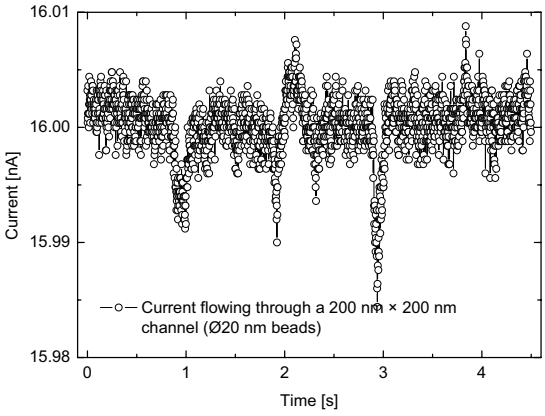

Figure 5.10: 20 nm diameter particles sensing in 200 nm × 200 nm cross-section, 3µm long channel.

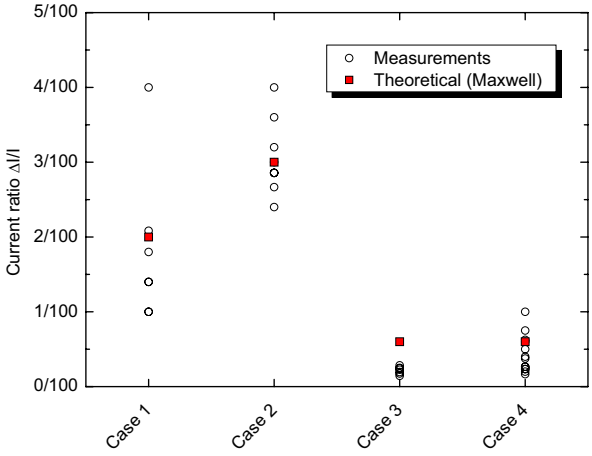

Figure 5.11: Theoretical versus measured relative current variation in: (case 1) 1 µm, (case 2) 500 nm, (case 3) 300 nm and (case 4) 200 nm channels.

- Using the fluorescence, we could observe that the nanochannel can be partially obstructed by particles binding on the nanochannel walls, however particles could still pass through the clog, which could be compared to a smaller channel diameter, thus to a higher current variation.
- The crossing of more than one particle at the same time because of the relatively high concentration of particles could also result in a higher ratio.
- The size distribution of the particles is also a parameter that could affect the variance of pulse amplitude.

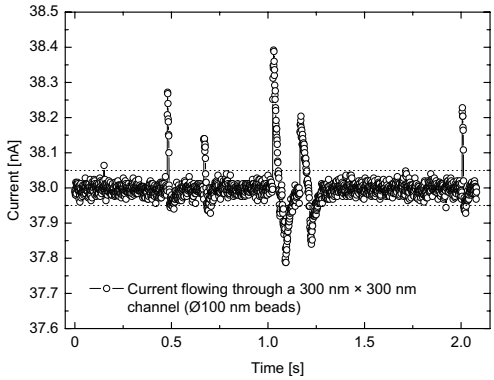

Figure 5.12: Positive current pulses.

On another hand, unlike in the literature, the current pulses in our case were usually preceded by a more important but non-proportional positive current pick as we can see in Figure 5.12. We actually don't have a satisfying explanation for these pulses, the electrical study should be pushed further to determine their exact origin.

5.3.4 DNA detection

Bacteriophage DNA, 165.65 kbp (Nippon Gene, Japan) sensing in 300 × 300 nm^2 channel has been achieved. The DNA solution was diluted to 40 pM in 10 mM Tris-HCl (pH 8), 1 mM EDTA, 0.1 M KCl buffer and labelled with YOYO-1 fluorescence dye (Molecular probes, Carlsbad, CA, USA). The concentration of YOYO-1 was a thousand times higher than that of DNA in the final solution. The applied DC voltage was 2 V. As we can see on the plots of Figure 5.13, the noise level is still too high to clearly distinguish the current pulses. However, using a low pass numerical filter we believe that we detect the presence of $\sim$ 150 pA amplitude and 20 ms duration pulse. Since DNA molecules optical detection is hardly achievable in 300 nm channel using the setup of Figure 5.1, we could not check the transit time and thus use filters during the current measurement. Moreover, the display system that we used (Tektronix Oscilloscope) did not allow high sampling frequency (2.5 kHz) for more than 1 s. Though, it is difficult to compare noise and pulses in a representative manner. Nevertheless, by comparing with the results obtained by Saleh *et al.* for λ-DNA molecules (48.502 bp) detection in a 200 × 200 nm^2 nanochannel (given in Figure 3.5) [18], we can see that the transit time and relative current variation ($\Delta I/I$) in our case are comparable.

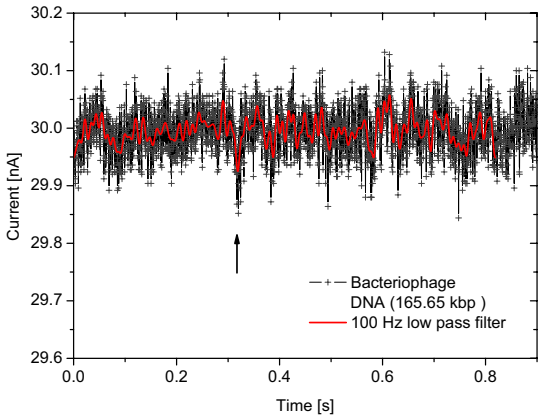

Figure 5.13: DNA (165.65 kbp) detection by resistive-pulse method.

DNA Molecule	**Channel size**	**Applied voltage**	**Pulse duration**	$\Delta I/I$	**N/S level**
Bacteriophage (165.65 kbp)	300 × 300 nm^2 3 µm	2 V	10-20 ms	3-5×10^{-3}	3.3×10^{-3}
λ-DNA (48.502 kbp)	200 × 200 nm^2 3 µm	0.4 V	2-10 ms	3×10^{-3} 6.6×10^{-3}	3.3×10^{-4}

Table 5.3: Bacteriophage DNA and λ-DNA detection in a nanochannel. Comparison of our parameters with those of O. A. Saleh [4].

Chapter 6

Conclusion

A microfluidic chip including a nanochannel for resistive-pulse detection has been developed, fabricated and characterized. Diverse technologies such as platinum sputtering and etching for the electrodes deposition, direct electron-beam writing and etching for 1 µm to 200 nm silicon nanostructures, SU-8 lithography for patterning the microstructures and PDMS moulding were successfully achieved for the fabrication of the device. 200 nm, 100 nm and 20 nm diameter beads have been detected through various cross-section nanochannels with a diameter ratio d/D from 0.2 to 0.066. The results were in compliance with the theoretical predictions.
For DNA detection, the results we obtained were promising. At the present time, our main limitation for DNA pulse clear visualization is the noise to signal ratio ($\sim 3.3 \times 10^{-3}$). Therefore, the next step to be solved is to decrease the noise level by using an adapted low-pass filter, and perhaps to test an other environment for performing the experiments. Indeed, too many apparatus operating in the same room might have disturbed our measurements.
The particles flow is achieved by means of pressure. Consequently, controlling the particles flow is hardly achievable. So far, electrophoresis has been ineffective but should be more deeply investigated using the 4 channels design. It should be possible to perform EP between the inlet reservoir and one of the measuring electrodes, then between the two inner electrodes.
Additionally, an array of nanochannels could be used as a filter in order to prevent big particles from reaching the detection nanochannel, thus avoiding its obstruction.
A real time acquisition system combined with fast processing is also necessary to perform a feedback control on the particle flow, *e.g.* LabView software in combination with a rapid A/D converter.
Once solved the above mentioned aspects, the next step will be the integration of the resistive-pulse detection in a more complex Lab-On-a-Chip device for bio-assays on DNA. In our case, for the single DNA molecule detection, isolation and trapping by combination of resistive-pulse detection method in the system developed by M. Kumemura *et al.* [2].

Tokyo, February 23, 2007

Mariam BENABDERRAZIK

Bibliography

[1] J. T. Mannion, C. H. Reccius, J. D. Cross, and H. G. Craighead. Conformational analysis of single DNA molecules undergoing entropically induced motion in nanochannels. *Biophysical Journal*, 90(12):4538–4545, 2006. doi: 10.1529/biophysj.105.074732.

[2] M. Kumemura, D. Collard, C. Yamahata, N. Sakaki, G. Hashiguchi, and H. Fujita. Single DNA molecule isolation and trapping in a microfluidic device. Submitted article, 2007.

[3] W. H. Coulter. Means for counting particles suspended in a fluid, 1953. US patent 2656508.

[4] O. A. Saleh. *A novel resistive pulse sensor for biological measurements*. Ph.D. thesis, Princeton University, 2003.

[5] S. Oh, J. S. Lee, K. H. Jeong, and L. P. Lee. Minimization of electrode polarization effect by nanogap electrodes for biosensor applications. In *MEMS'03, the Sixteenth IEEE Annual International Conference on Micro Electro Mechanical Systems*, page 52, Kyoto, Japan, 2003. doi: 10.1109/MEMSYS.2003.1189685.

[6] P. Mirtaheri, S. Grimnes, and O. G. Martinsen. Electrode polarization impedance in weak nacl aqueous solutions. *IEEE Transactions on Biomedical Engineering*, 52(12):2093–2099, 2005. doi: 10.1109/TBME.2005.857639.

[7] J. C. Maxwell. *A Treatise on Electricity and Magnetism*, volume 1. Clarendon, Oxflord, 1904.

[8] J. W. Rayleigh. On the influence of obstacles arranged in rectangular order upon the properties of a medium. *Philosophical Magazine*, 34:481–502, 1892.

[9] R. W. Deblois and C. P. Bean. Counting and sizing of submicron particles by resistive pulse technique. *Review of Scientific Instruments*, 41(7):909–916, 1970. doi: 10.1063/1.1684724.

[10] D. Li. *Electrokinetics in Microfluidics*, volume 2 of *Interface Science and Technology*. Elsevier Academic Press, first edition, 2004.

[11] Coulter counter apparatus. Beckman Coulter Inc., http://www.beckmancoulter.com/.

[12] S. M. Bezrukov, I. Vodyanoy, and V. A. Parsegian. Counting polymers moving through a single-ion channel. *Nature*, 370(6487):279–281, 1994. doi: 10.1038/370279a0.

[13] L. Sun and R. M. Crooks. Single carbon nanotube membranes: A well-defined model for studying mass transport through nanoporous materials. *Journal of the American Chemical Society*, 122(49):12340–12345, 2000. doi: 10.1021/ja002429w.

[14] R. R. Henriquez, T. Ito, L. Sun, and R. M. Crooks. The resurgence of coulter counting for analyzing nanoscale objects. *Analyst*, 129(6):478–482, 2004. doi: 10.1039/b404251b.

[15] J. Li, D. Stein, C. McMullan, D. Branton, M. J. Aziz, and J. A. Golovchenko. Ion-beam sculpting at nanometre length scales. *Nature*, 412(6843):166–169, 2001. doi: 10.1038/35084037.

[16] H. Chang, F. Kosari, G. Andreadakis, M. A. Alam, G. Vasmatzis, and R. Bashir. DNA-mediated fluctuations in ionic current through silicon oxide nanopore channels. *Nano Letters*, 4(8):1551–1556, 2004. doi: 10.1021/nl049267c.

[17] C. C. Harrell, Y. Choi, L. P. Horne, L. A. Baker, Z. S. Siwy, and C. R. Martin. Resistive-pulse DNA detection with a conical nanopore sensor. *Langmuir*, 22(25):10837–10843, 2006. doi: 10.1021/la061234k.

[18] O. A. Saleh and L. L. Sohn. An artificial nanopore for molecular sensing. *Nano Letters*, 3(1):37–38, 2003. doi: 10.1021/nl0255202.

[19] O. A. Saleh and L. L. Sohn. Direct detection of antibody-antigen binding using an on-chip artificial pore. *Proceedings of the National Academy of Sciences of the United States of America*, 100(3):820–824, 2003. doi: 10.1073/pnas.0337563100.

[20] O. A. Saleh and L. L. Sohn. Biological sensing with an on-chip resistive pulse analyzer. In *EMBC 2004, 26th Annual International Conference of the Engineering in Medicine and Biology Society*, pages 2568 – 2570, San Francisco, CA, USA, 2004. IEEE. doi: 10.1109/IEMBS.2004.1403738.

[21] A. Carbonaro and L. L. Sohn. A resistive-pulse sensor chip for multianalyte immunoassays. *Lab on a Chip*, 5(10):1155–1160, 2005. doi: 10.1039/b504827c.

Appendix A

- Fabrication flow process for Silicon nanochannel and SU-8 microstructures
- Fabrication flow process for Platinum electrodes
- Datasheets of SU-8 photoresist (MicroChem)
- Datasheets of Sylgard® 184 (Dow Corning)
- Datasheets of fluorescent microspheres (Molecular Probes)
- Datasheets of Keithley 428 Programmable Current Amplifier

Author:	Christophe Yamahata
Date:	November 20th, 2006
Process name:	Nanochannel & Microchannel
Short description:	Fabrication of a mould for PDMS nanochannel. SU-8 resist is used for microstructures, while the nanostructures are obtained by direct e-beam writing and ICP-RIE of silicon.
Process type:	Silicon micromachining
Substrate:	Standard Si wafer, 381 µm thick
Mask:	Direct writing (e-beam) + Mask for negative resist (SU-8).
Keywords:	SU-8, ICP, PDMS

Process flow

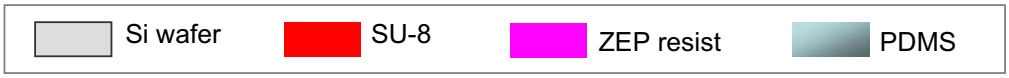

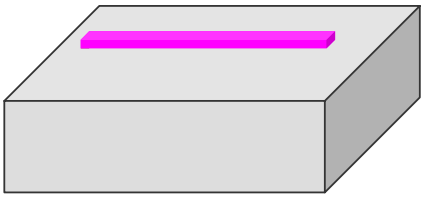

1. Direct e-beam writing (mask #1, ZEP 520) + O_2 plasma ashing

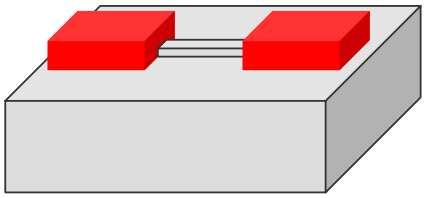

3. SU-8 lithography (mask #2)

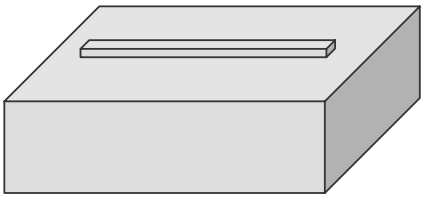

2. ICP-RIE (200 nm) + ZEP removal

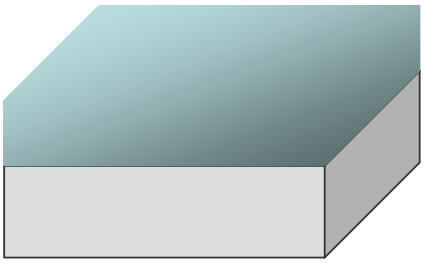

4. PDMS moulding

Photograph of the fabricated structures

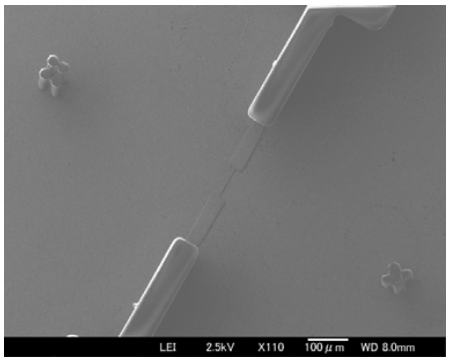

SU-8 microstructures and Si nanochannel (~ 100-150 µm thick SU-8 structures were obtained)

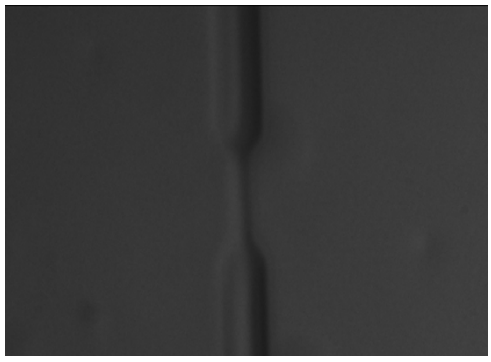

PDMS nanochannel observed with DUV microscope (200 nm × 200 nm × 3 µm).

Nanostructures (direct e-beam writing)

Step	Process		Comment
1	Substrate Selection Silicon Wafer	Diameter: 3'' Thickness: 275µm -775 µm Crystallographic Orientation: () Doping: (-type) Resistivity: Ωcm	Thickness of 381 µm was chosen for direct e-beam writing
2	Surface Cleaning SPM (Piranha) Process (H_2SO_4/H_2O_2)	*Removal of particles and organic contamination.* Chemicals: H_2SO_4 (96%) Kanto Chemical Co. Inc. H_2O_2 (30%) Kanto Chemical Co. Inc. Ratio: H_2SO_4: H_2O_2 (2:1) • Cleaning Time: 5 – 10 min Rinsing with DI water! Remarks: *No heating needed (exothermic reaction). Be careful solution is hot (~120 °C) Formation of oxide layer on silicon.*	Time: 5 min

3	EB Lithography
	Resist Coating
	(HMDS)
		Spincoater Mikasa 1H-D7 (1F & 3F)
		Chemicals: HMDS primer (adhesion layer)
		Time:
		t1=5 s; t2=5 s; t3=5 s; t4=40 s t5= 5s;
		Rotational speed:
		r1=500 rpm; r2=4000 rpm;
		 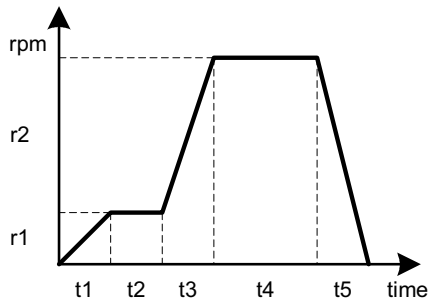
			Time:
			t1= 5 s
			t2= 5 s
			t3= 5 s
			t4= 60 s
			t5= 6 s
			Rotation:
			r1= 500 rpm
			r2= 4000 rpm

4	EB Lithography
	Resist Coating
	(ZEP 520-A)
		Spincoater Mikasa 1H-D7 (1F & 3F)
		Resist: ZEP 520-A EB-resist
		Time:
		t1=5 s; t2=5 s; t3=5 s; t4=40 s t5= 5s;
		Rotational speed:
		r1=500 rpm; r2=4000 rpm;
		 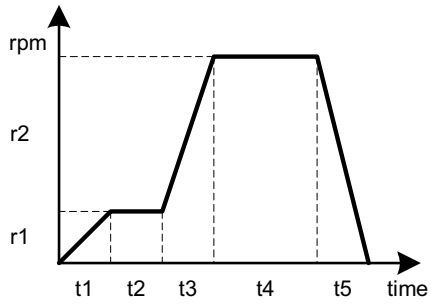
			Time:
			t1= 5 s
			t2= 5 s
			t3= 5 s
			t4= 60 s
			t5= 6 s
			Rotation:
			r1= 500 rpm
			r2= 4000 rpm

<table>
<tr><td>5</td><td>EB Lithography
Pre-Bake
(ZEP 520-A)</td><td>Digital Hot Plate IUCHI PMC-720 (1F & 3F)
Resist: ZEP 520-A EB-resist
Temperature and Time:
ZEP 520-A resist (4000 rpm): 180 °C, 5 min</td><td>Temp= 180°C
Time= 5 min</td></tr>
<tr><td>6</td><td>EB Lithography
EB Exposure
(ADVANTEST EB)</td><td>Equipment: ADVANTEST EB Machine
Dose: 88 μC/cm^2
Acceleration Voltage: 50 keV</td><td>A dose of 88 μC/cm^2 on ZEP 520-A was optimal to obtain ~ 200 nm wide structures</td></tr>
<tr><td>7</td><td>EB Lithography
Development
(ZEP 520-A)</td><td>Chemicals: ZED N50, ZMD-B and IPA
Development in ZED N50:
ZEP 520-A (4000 rpm): ~ 4 min 30 s
Rinse in ZMD-B : 1 min
Rinse in DI water!</td><td>Time= 4 min 30s</td></tr>
<tr><td>8</td><td>Etching
RIE
(Oxygen Plasma Ashing)</td><td>RIE system SAMCO– 10NR (1F)
Removal of photoresist or FC-polymers.
O_2 flow 50 sccm
RF power 50 W
Pressure 10 Pa</td><td>50 sccm O_2,
10 Pa, 50 W
Time: 10 sec</td></tr>
<tr><td>9</td><td>Etching
ICP-RIE (DRIE)
(STS ICP)</td><td>STS ICP (3F)
SOI PROCESS: Anisotropic etching of silicon with well-defined profile.
<table><tr><th>Parameters</th><th>Etch</th><th>Passivation</th></tr><tr><td>C_4F_8 [sccm]</td><td>0</td><td>100</td></tr><tr><td>SF_6 [sccm]</td><td>110</td><td>0</td></tr><tr><td>O_2 [sccm]</td><td>13</td><td>0</td></tr><tr><td>Ar [sccm]</td><td>0</td><td>0</td></tr><tr><td>t [s]</td><td>8</td><td>5</td></tr><tr><td>p [mTorr]</td><td colspan="2">5</td></tr><tr><td>APC [%]</td><td colspan="2">60</td></tr><tr><td>13.56 MHz Generator [W]</td><td>600</td><td>600</td></tr><tr><td>Platen generator</td><td colspan="2">380 kHz</td></tr><tr><td>Platen generator [W]</td><td>40</td><td>0</td></tr><tr><td>He [sccm]</td><td colspan="2">10 – 40 sccm</td></tr><tr><td>He [Torr]</td><td colspan="2">9.8</td></tr></table>Etch rates:
Silicon: ~1 μm /min
Photoresist: xx nm/min
Silicon Nitride: xx nm/min
Silicon Oxide: xx nm/min</td><td>Process called “SOI 10040”
(Si etching:
~1 μm/15min)

No.cycles=
Time= 3 min
(~200 nm deep)</td></tr>
<tr><td>10</td><td>EB Lithography
Resist Removal
(ZEP 520-A)</td><td>Chemicals: ZDMAC
Removal of resist by ZDMAC!
EB-Resist: ZEP 520-A
Temperature and Time:
ZEP 520-A resist (4000 rpm): 80 °C, 5 min</td><td>Temp= 80 °C
Time= 5 min</td></tr>
<tr><td>11</td><td>Etching
RIE
(Oxygen Plasma Ashing)</td><td>RIE system SAMCO– 10NR (1F)
Removal of photoresist or FC-polymers.
O_2 flow 100 sccm
RF power 50 W
Pressure 10 Pa</td><td>100 sccm O_2,
10 Pa, 50 W
Time: 1 or 2 min

This final cleaning with plasma can be done if necessary</td></tr>
</table>

Microstructures (SU-8)

Step	Process		Comment
1	Surface Cleaning SPM (Piranha) Process (H_2SO_4/H_2O_2)	*Removal of particles and organic contamination.* Chemicals: H_2SO_4 (96%) Kanto Chemical Co. Inc. H_2O_2 (30%) Kanto Chemical Co. Inc. Ratio: H_2SO_4: H_2O_2 (2:1) • Cleaning Time: 5 – 10 min Rinsing with DI water! Remarks: *No heating needed (exothermic reaction). Be careful solution is hot (~120 °C) Formation of oxide layer on silicon.*	Time: 20 min
2	Optical Lithography Substrate Pretreat Negative resist (SU-8 2050)	Digital Hot Plate IUCHI PMC-720 (1F & 3F) Resist: SU-8 (Microchem Nano™ SU-8 2000) Temperature and Time: Si substrate : 200 °C, 5 min Cooling: 5 min	Temp= 200 °C Time= 5 min

3	Optical Lithography
	Resist Coating
	Negative resist
	(SU-8 2050)
		Spincoater Mikasa 1H-D7 (1F & 3F)
		Resist: SU-8 2000 negative photoresist
		(Microchem Nano™ SU-8 2000)
		Time:
		t1=5 s; t2=10 s; t3=5 s; t4=30 s t5= 5s;
		Rotational speed:
		r1=500 rpm; r2=1500 rpm;
		 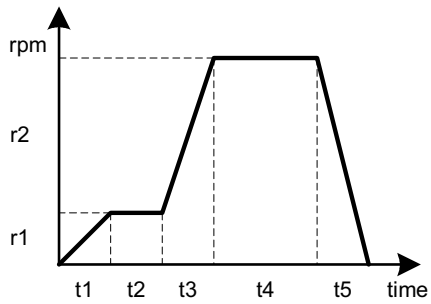
		
			Time:
			t1= 5 s
			t2= 10 s
			t3= 5 s
			t4= 30 s
			t5= 5 s
			Rotation:
			r1= 500 rpm
			r2= 1500 rpm
			Check the parameters provided by Microchem to adjust the thickness

4	Optical Lithography Soft-Bake Negative resist (SU-8 2050)	Digital Hot Plate IUCHI PMC-720 (1F & 3F) Resist: SU-8 2000 negative photoresist (Microchem Nano™ SU-8 2000) Temperature and Time: 1st soft bake: 65 °C, 4 min 2nd soft bake: 95 °C, 20 min Cooling: 20 min ~ 1 hour	1) 4 min @ 65 °C 2) 20 min@ 95°C Cooling: 20 min
5	Optical Lithography Exposure (UNION Aligner NEW)	UNION Mask Aligner NEW (1F) Hg lamp: xx mW/cm^2 Exposure time: <u>Negative resist</u> • SU-8 2050 (1500 rpm) ~ 30 s Remarks: *Exposure time is an indication and can vary depending on the state of the lamp.*	Time= 30 s Gap alignment: 100 μm
6	Lithography: Post-Bake Negative resist (SU-8 2050)	Digital Hot Plate IUCHI PMC-720 (1F & 3F) Resist: SU-8 2000 negative photoresist (Microchem Nano™ SU-8 2000) Temperature and Time: 1st post bake: 65 °C, 1 min 2nd post bake: 95 °C, 7 min	1) 1 min @ 65 °C 2) 7 min@ 95°C Cooling: 1 hour

		Cooling: 20 min ~ 1 hour	
7	Optical Lithography Development Negative resist (SU-8 2050)	Chemicals: SU-8 developer Development time: SU-8 2050 (1500 rpm): ~ 7 min Remarks: Development time is an indication! Strong agitation is recommended to obtain high aspect ratio.	Time= 15 min
8	Surface Cleaning Ultrasonic Process (Acetone, Ethanol, IPA)	1) 2 baths of IPA 2) DI water Remark: *If a white film is produced, this is an indication that the substrate has been under developed.*	Go to previous step if a white film is produced.
9	Lithography: Hard-Bake (cure) Negative resist (SU-8 2050)	Digital Hot Plate IUCHI PMC-720 (1F & 3F) Resist: SU-8 2000 negative photoresist (Microchem Nano^{TM} SU-8 2000) Temperature and Time: SU-8 2050 (1500 rpm): 150-200 ^{o}C, … min Remark: *This step is optional*. *SU-8 has good mechanical properties, therefore hard bakes are usually not required. For applications where the resist is to be left as part of the final device, the resist may be hard baked.*	Temp= 200 ^{o}C Time= 5 min

Platinum electrodes on microscope cover glass

C. Yamahata & M. Benabderrazik, October 2006 (based on the process of F. Gillot)

Step	Process		Comment
Substrate cleaning			
1	Substrate Selection Glass Slides	Micro Cover Glass (Matsunami NEO) Size: 24 mm x 36 mm Thickness: 0.12 mm ~0.17 mm	
2	Surface Cleaning SPM (Piranha) Process (H_2SO_4/H_2O_2)	*Removal of particles and organic contamination.* Chemicals: H_2SO_4 (96%) Kanto Chemical Co. Inc. H_2O_2 (30%) Kanto Chemical Co. Inc. Ratio: H_2SO_4: H_2O_2 (1:1) • Cleaning Time: 5 – 10 min Rinsing with DI water! Remarks: *No heating needed (exothermic reaction). Be careful solution is hot (~120 °C) Formation of oxide layer on silicon.*	Ratio: 200 cL / 200 cL Time: 5min (done in 1F-CR)
Sputtering			
3	Deposition Sputtering	Ti / Pt / SiO_2	Use F. Gillot's parameters
Lithography			

4	Optical Lithography
	Priming
	(HMDS)
		Spincoater Mikasa 1H-D7 (1F)
		Chemicals: HMDS primer
		Time:
		t1=5 s; t2=5 s; t3=5 s; t4=40 s t5= 5s;
		Rotational speed:
		r1=500 rpm; r2=4000 rpm;
		 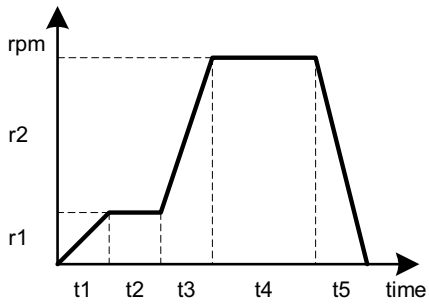
		
			Time:
			t1= 5 s
			t2= 10 s
			Rotation:
			r1= 500 rpm
			
			Put HMDS when spincoater speed is 500 rpm.
			
			(done in 1F-CR)

5	Optical Lithography
	Resist Coating
	Positive resist
	(S1805)
		Spincoater Mikasa 1H-D7 (1F & 3F)
		Resist: S1805 positive photoresist
		Time:
		t1=5 s; t2=5 s; t3=5 s; t4=40 s t5= 5s;
		Rotational speed:
		r1=500 rpm; r2=4000 rpm;
			Time:
			t1= 5 s
			t2= 10 s
			t3= 5 s
			t4= 30 s
			t5= 5 s
			Rotation:
			r1= 500 rpm
			r2= 3000 rpm

		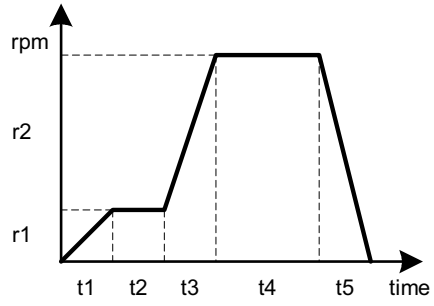	
6	Optical Lithography Pre-Bake Positive resist (S1805)	Digital Hot Plate IUCHI PMC-720 (1F & 3F) Resist: S1805 positive photoresist Temperature and Time: S1805 resist (3000 rpm): 90 °C, ~10 min S1805 resist (4000 rpm): 90 °C, ~10 min Remark: *By using BEMCOAT increase bake temperature 15 °C to 105 °C.*	Temp= 60 °C Time= 3 min No bemcoat.
7	Optical Lithography Exposure (UNION Aligner NEW)	UNION Mask Aligner NEW (1F) Hg lamp: xx mW/cm2 Exposure time: Positive resist • S1818 (4000 rpm) ~ 4 s - 5 s • S1805 (4000 rpm) ~ 1 s - 2 s Negative resist • ZPN (3000 rpm) ~ x-x s • ZPN (4000 rpm) ~ x-x s Remarks: Exposure time is an indication and can vary depending on the state of the lamp.	Time= 1.5 s (300 W)
8	Optical Lithography Development Positive resist (S1805)	Chemicals: NMD3 developer Development time: S1805 resist (3000 rpm): ~ 40 s - 60 s S1805 resist (4000 rpm): ~ 40 s - 60 s Remarks: *Development time is an indication!*	Time= 60 s 50 sec without agitation followed by 10 sec agitation. Rinse in DI water. Dry carefully.
9	Lithography: Post-Bake Positive resist (S1805)	Digital Hot Plate IUCHI PMC-720 (1F & 3F) Resist: S1805 positive photoresist Temperature and Time: S1805 resist (3000 rpm): 120 °C, >5 min S1805 resist (4000 rpm): 120 °C, >5 min Remark: *By using BEMCOAT increase bake temperature 15 °C to 135 °C.*	Temp= 130 °C Time= 5 min No bemcoat.
RIE			
10	Etching RIE		

MICRO CHEM

www.microchem.com

SU-8 2000

Permanent Epoxy Negative Photoresist

PROCESSING GUIDELINES FOR:

SU-8 2100 and SU-8 2150

SU-8 2000 is a high contrast, epoxy based photoresist designed for micromachining and other microelectronic applications, where a thick, chemically and thermally stable image is desired. SU-8 2000 is an improved formulation of SU-8, which has been widely used by MEMS producers for many years. The use of a faster drying, more polar solvent system results in improved coating quality and increases process throughput. SU-8 2000 is available in twelve standard viscosities. Film thicknesses of 0.5 to >200 microns can be achieved with a single coat process. The exposed and subsequently thermally cross-linked portions of the film are rendered insoluble to liquid developers. SU-8 2000 has excellent imaging characteristics and is capable of producing very high aspect ratio structures. SU-8 2000 has very high optical transmission above 360 nm, which makes it ideally suited for imaging near vertical sidewalls in very thick films. SU-8 2000 is best suited for permanent applications where it is imaged, cured and left on the device.

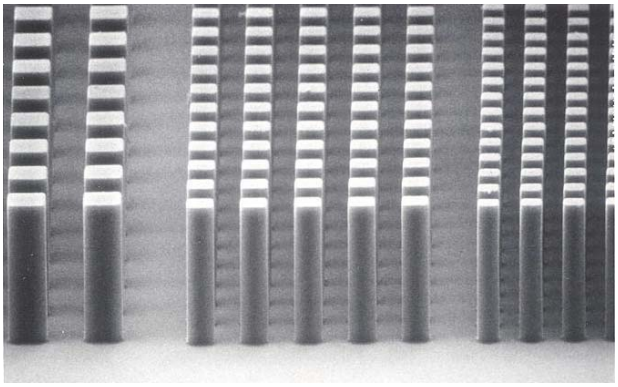

10 um features, 50 um SU-8 2000 coating

SU-8 2000 Features

- High aspect ratio imaging
- 0.5 to > 200 μm film thickness in a single coat
- Improved coating properties
- Faster drying for increased throughput
- Near UV (350-400 nm) processing
- Vertical sidewalls

Process Flow

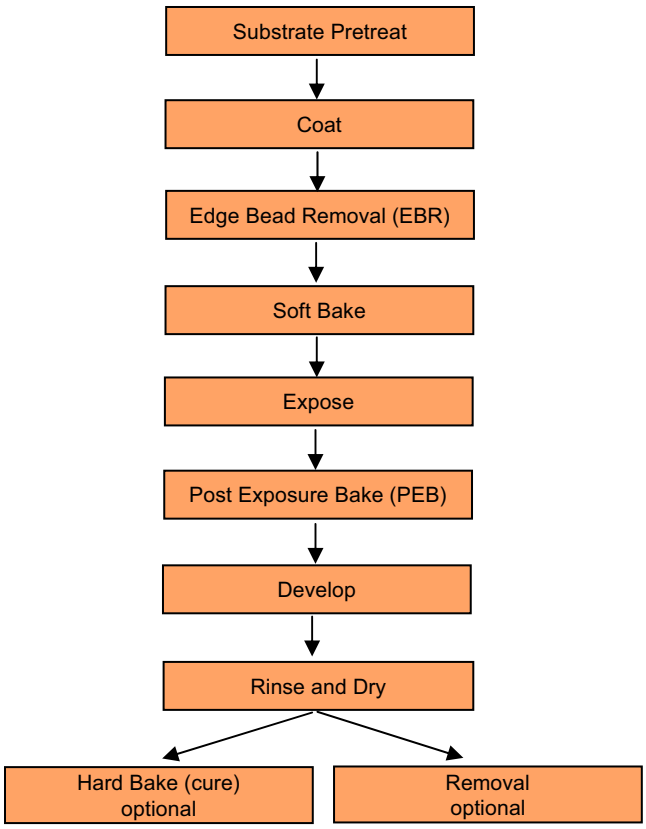

Processing Guidelines

SU-8 2000 photoresist is most commonly exposed with conventional UV (350-400 nm) radiation, although i-line (365 nm) is the recommended wavelength. SU-8 2000 may also be exposed with e-beam or x-ray radiation. Upon exposure, cross-linking proceeds in two steps (1) formation of a strong acid during the exposure step, followed by (2) acid-catalyzed, thermally driven epoxy cross-linking during the post exposure bake (PEB) step. A normal process is: spin coat, soft bake, expose, PEB, followed by develop. A controlled hard bake is recommended to further cross-link the imaged SU-8 2000 structures when they will remain as part of the device. The entire process should be optimized for the specific application. The baseline information presented here is meant to be used as a starting point for determining a process.

Substrate Preparation

To obtain maximum process reliability, substrates should be clean and dry prior to applying SU-8 2000 resist. For best results, substrates should be cleaned with a piranha wet etch (using H_2SO_4 & H_2O_2) followed by a de-ionized water rinse. Substrates may also be cleaned using reactive ion etching (RIE) or any barrel asher supplied with oxygen. Adhesion promoters are typically not required. For applications that include electroplating, a pre-treatment of the substrate with MCC Primer 80/20 (HMDS) is recommended.

Coat

SU-8 2000 resists are available in twelve standard viscosities. This processing guideline document addresses two products: SU-8 2100 and SU-8 2150. Figure 1. provides the information required to select the appropriate SU-8 2000 resist and spin conditions to achieve the desired film thickness.

Recommended Program

1.) Dispense 1ml of resist for each inch (25mm) of substrate diameter.
2.) Spin at 500 rpm for 5-10 seconds with acceleration of 100 rpm/second.
3.) Spin at 2000 rpm for 30 seconds with acceleration of 300 rpm/second.

Figure 1. SU-8 2000 Spin Speed versus Thickness

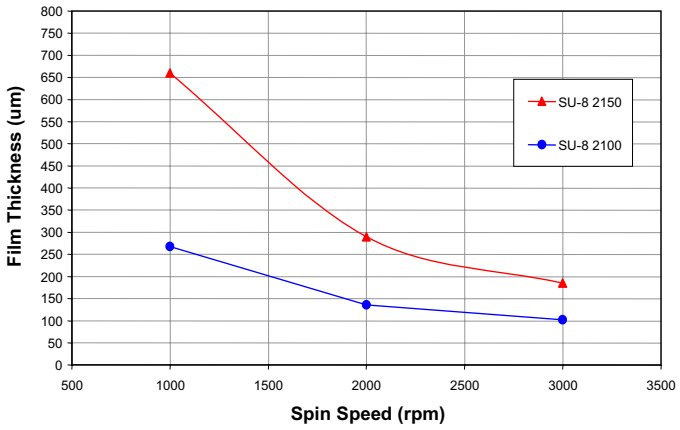

Table 1. SU-8 2000 Viscosity

SU-8 2000	% Solids	Viscosity (cSt)	Density (g/ml)
2100	75.00	45000	1.237
2150	76.75	80000	1.238

Edge Bead Removal (EBR)

During the spin coat process step, a build up of photoresist may occur on the edge of the substrate. In order to minimize contamination of the hotplate, this thick bead should be removed. This can be accomplished by using a small stream of solvent (MicroChem's EBR PG) at the edge of the wafer either at the top or from the bottom. Most automated spin coaters now have this feature and can be programmed to do this automatically.

By removing any edge bead, the photomask can be placed into close contact with the wafer, resulting in improved resolution and aspect ratio.

Soft Bake

A level hotplate with good thermal control and uniformity is recommended for use during the Soft Bake step of the process. Convection ovens are not recommended. During convection oven baking, a skin may form on the resist. This skin can inhibit the evolution of solvent, resulting in incomplete drying of the film and/or extended bake times. Table 2. shows the recommended Soft Bake temperatures and times for the various SU-8 2000 products at selected film thicknesses.

Note: *To optimize the baking times/conditions, remove the wafer from the hotplate after the prescribed time and allow it to cool to room temperature. Then, return the wafer to the hotplate. If the film 'wrinkles', leave the wafer on the hotplate for a few more minutes. Repeat the cool-down and heat-up cycle until 'wrinkles' are no longer seen in the film.*

THICKNESS	SOFT BAKE TIMES	
	(65°C)*	(95°C)
microns	minutes	minutes
100 - 150	5	20 - 30
160 - 225	5 - 7	30 - 45
230 - 270	7	45 - 60
280 - 550	7 - 10	60 - 120

Table 2. Soft Bake Times

Optical Parameters

The dispersion curve and Cauchy coefficients are shown in Figure 3. This information is useful for film thickness measurements based on ellipsometry and other optical measurements.

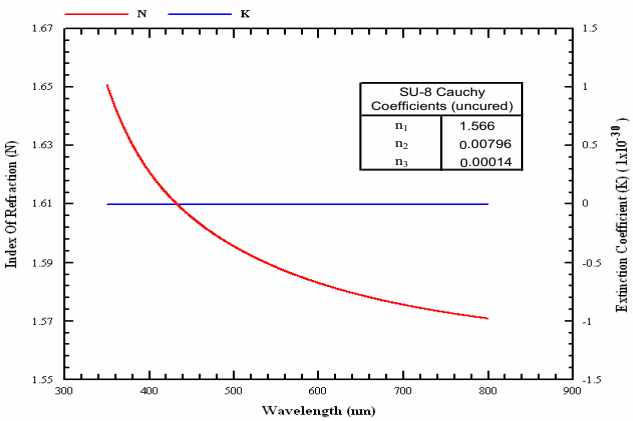

Figure 3. Cauchy Coefficients

Exposure

To obtain vertical sidewalls in the SU-8 2000 resist, we recommend the use of a long pass filter to eliminate UV radiation below 350 nm. With the recommended filter (PL-360-LP) from Omega Optical (www.omegafilters.com) or Asahi Technoglass filters V-42 plus UV-D35 (www.atgc.co.jp), an increase in exposure time of approximately 40% is required to reach the optimum exposure dose.

Note: *With optimal exposure, a visible latent image will be seen in the film within 5-15 seconds after being placed on the PEB hotplate and not before. An exposure matrix experiment should be performed to determine the optimum dosage.*

THICKNESS microns	EXPOSURE ENERGY mJ/cm^2
100 - 150	240 - 260
160 - 225	260 - 350
230 - 270	350 - 370
280 - 550	370 - 600

Table 3. Exposure Dose

	RELATIVE DOSE
Silicon	1X
Glass	1.5X
Pyrex	1.5X
Indium Tin Oxide	1.5X
Silicon Nitride	1.5 - 2X
Gold	1.5 - 2X
Aluminum	1.5 - 2X
Nickel Iron	1.5 - 2X
Copper	1.5 - 2X
Nickel	1.5 - 2X
Titanium	1.5 - 2X

Table 4. Exposure Doses for Various Substrates

Post Exposure Bake (PEB)

PEB should take place directly after exposure. Table 5. shows the recommended times and temperatures

Note: *After 1 minute of PEB at 95°C, an image of the mask should be visible in the SU-8 2000 photoresist coating. If no visible latent image is seen during or after PEB this means that there was insufficient exposure, heating or both.*

THICKNESS microns	PEB TIME (65°C)* minutes	PEB TIME (95°C) minutes
100 - 150	5	10 - 12
160 - 225	5	12 - 15
230 - 270	5	15 - 20
280 - 550	5	20 - 30

* Optional step for stress reduction

Table 5. Post Exposure Bake Times

Development

SU-8 2000 photoresist has been designed for use in immersion, spray or spray-puddle processes with MicroChem's SU-8 developer. Other solvent based developers such as ethyl lactate and diacetone alcohol may also be used. Strong agitation is recommended when developing high aspect ratio and/or thick film structures. The recommended development times for immersion processes are given in Table 6. These development times are approximate, since actual dissolution rates can vary widely as a function of agitation

Note: *The use of an ultrasonic or megasonic bath may be helpful when developing out via or hole patterns or structures with tight pitch.*

THICKNESS microns	DEVELOPMENT TIME minutes
100 - 150	10 - 15
160 - 225	15 - 17
230 - 270	17 - 20
280 - 550	20 - 30

Table 6. Development Times for SU-8 Developer

Rinse and Dry

When using SU-8 developer, spray and wash the developed image with fresh solution for approximately 10 seconds, followed by a second spray/wash with Isopropyl Alcohol (IPA) for another 10 seconds. Air dry with filtered, pressurized air or nitrogen.

Note: *A white film produced during IPA rinse is an indication of underdevelopment of the unexposed photoresist. Simply immerse or spray the substrate with additional SU-8 developer to remove the white film and complete the development process. Repeat the rinse step.*

The use of an ultrasonic or megasonic bath will energize the solvent and allow for more effective development of the unexposed resist.

Physical Properties

(Approximate values)

Adhesion Strength (mPa) Silicon/Glass/Glass & HMDS	38/35/35
Glass Transition Temperature (Tg °C), tan δ peak	210
Thermal Stability (°C @ 5% wt. loss)	315
Thermal Conductivity (W/mK)	0.3
Coeff. of Thermal Expansion (CTE ppm)	52
Tensile Strength (Mpa)	60
Elongation at break (εb %)	6.5
Young's Modulus (Gpa)	2.0
Dielectric Constant @ 10MHz	3.2
Water Absorption (% 86/85 RH)	0.65

Table 7. Physical Propeties

Optical Properties

Figure 4. Optical Transmittance

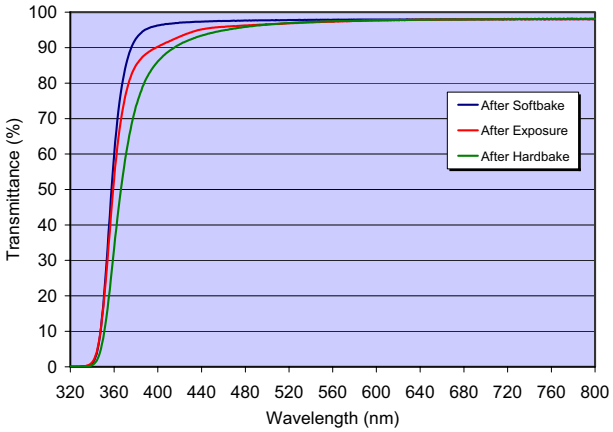

Process conditions for Figure 4.
Softbake: 5 minutes at 95°C
Exposure: 180 mJ/cm^2
Hardbake: 30 minutes at 300°C

Hard Bake (cure)

SU-8 2000 has good mechanical properties. However, for applications where the imaged resist is to be left as part of the final device, a hard bake can be incorporated into the process. This is generally only required if the final device or part is to be subject to thermal processing during regular operation. A hard bake or final cure step is added to ensure that SU-8 2000 properties do not change in actual use. SU-8 2000 is a thermal resin and as such its properties can continue to change when exposed to a higher temperature than previously encountered. We recommend using a final bake temperature 10°C higher than the maximum expected device operating temperature. Depending on the degree of cure required, a bake temperature in the range of 150°C to 250°C and for a time between 5 and 30 minutes is typically used.

Note: *The hard bake step is also useful for annealing any surface cracks that may be evident after development. The recommended step is to bake at 150°C for a couple of minutes. This applies to all film thicknesses.*

Removal

SU-8 2000 has been designed as a permanent, highly cross-linked epoxy material and it is extremely difficult to remove it with conventional solvent based resist strippers. MicroChem's Remover PG will swell and lift off minimally cross-linked SU-8 2000. However, if OmniCoat (30-100 nm) has been applied, immersion in Remover PG can effect a clean and thorough Lift-Off of the SU-8 2000 material. Fully cured or hard baked SU-8 2000 cannot be removed without the use of OmniCoat.

To remove minimally cross-linked SU-8 2000, or when using Omnicoat: Heat the Remover PG bath to 50-80°C and immerse the substrates for 30-90 minutes. Actual strip time will depend on resist thickness and cross-link density For more information on MicroChem Omnicoat and Remover PG please see the relevant product data sheets.

To re-work fully cross-linked SU-8 2000: Wafers can be stripped using oxidizing acid solutions such as piranha etch, plasma ash, RIE, laser ablation and pyrolysis.

Plasma Removal

RIE 200W, 80 sccm O2, 8 sccm CF4, 100mTorr, 10°C

Storage

Store SU-8 2000 resists upright and in tightly closed containers in a cool, dry environment away from direct sunlight at a temperature of 40-70°F (4-21°C). Store away from light, acids, heat and sources of ignition. Shelf life is twelve months from date of manufacture.

Disposal

SU-8 2000 resists may be included with other waste containing similar organic solvents to be discarded for destruction or reclaim in accordance with local state and federal regulations. It is the responsibility of the customer to ensure the disposal of SU-8 2000 resists and residues made in observance all federal, state, and local environmental regulations.

Environmental, Health and Safety

Consult the product Material Safety Data Sheet before working with SU-8 2000 resists. Handle with care. Wear chemical goggles, chemical gloves and suitable protective clothing when handling SU-8 2000 resists. Do not get into eyes, or onto skin or clothing. Use with adequate ventilation to avoid breathing vapors or mist. In case of contact with skin, wash affected area with soap and water. In case of contact with eyes, rinse immediately with water and flush for 15 minutes lifting eyelids frequently. Get emergency medical assistance.

The information is based on our experience and is, we believe to be reliable, but may not be complete. We make no guarantee or warranty, expressed or implied, regarding the information, use, handling, storage, or possession of these products, or the application of any process described herein or the results desired, since the conditions of use and handling of these products are beyond our control.

Disclaimer

Notwithstanding anything to the contrary contained in any sales documentation, e.g., purchase order forms, all sales are made on the following conditions:
All information contained in any MicroChem product literature reflects MicroChem's current knowledge on the subject and is, we believe, reliable. It is offered solely to provide possible suggestions for customer's own experiments and is not a substitute for any testing by customer to determine the suitability of any of MicroChem products for any particular purpose. This information may be subject to revision as new knowledge and experience becomes available, but MicroChem assumes no obligation to update or revise any data previously furnished to a customer; and if currency of data becomes an issue, customer should contact MicroChem requesting updates. Since MicroChem cannot anticipate all variations in actual end uses or in actual end-use conditions, it makes no claims, representations or warranties, express or implied including, without limitation any warranty of merchantability or fitness for a particular purpose; and customer waives all of the same. MicroChem expressly disclaims any responsibility or liability and assumes no responsibility or liability in connection with any use of this information including, without limitation, any use, handling, storage or possession of any MicroChem products, or the application of any process described herein or the results desired or anything relating to the design of the customer's products. Nothing in this publication is to be considered as a license to operate under or a recommendation to infringe any patent right.

Caution

This product is not designed or manufactured for, nor is it intended for use in any medical device or for any other medical application. Do not use this product in any medical applications [including, without limitation, any permanent implantation in the human body or any animals (other than laboratory animals used for experimental purposes), or contact with internal body fluids or tissues] unless otherwise expressly and specifically provided for in a written contract between MCC and the customer. The complete MicroChem Medical Disclaimer Statement is available upon request or on the MicroChem website at www.microchem.com.

1254 Chestnut St.
Newton, MA 02464
PHONE: 617.965.5511
FAX: 617.965.5818
EMAIL: sales@ microchem.com
www.microchem.com

Product Information

SYLGARD® 184 Silicone Elastomer

FEATURES

- Two-part, 10:1 mixing ratio
- Medium viscosity
- Room temperature cure or rapid heat cure
- Addition cure system: no cure by-products
- Stable and flexible from -50°C (-58°F) to +200°C (392°F)
- Clear
- Flexible rubber - protects against mechanical shock and thermal cycling stress at components
- Excellent dielectric properties

Optically clear elastomer

APPLICATIONS

- Designed to protect against moisture, environmental attack, mechanical and thermal shock as well as vibration especially when optically clear product is required.
- Typical applications include: encapsulation of amplifiers, coils, connectors, circuit boards, equipment modules, ferrite cores, solar cells and transformers.

TYPICAL PROPERTIES

Specification writers: These values are not intended for use in preparing specifications. Please contact your local Dow Corning sales representative prior to writing specifications on this product.

CTM*	ASTM*	Property	Unit	Value
		As supplied		
0050	D1084	Viscosity at 23°C (Base)[1]	mPa.s	5500
		Mixing ratio by weight (Base:Curing Agent)		10:1
0050	D1084	Viscosity at 23°C, immediately after mixing with Curing Agent	mPa.s	4000
0055	D1824	Pot life at 23°C[2]	hours	2
		Physical properties, cured 4 hours at 65°C		
0176		Color		Clear
0099	D2240	Durometer hardness, Shore A		50
0137A	D412	Tensile strength	MPa	7.1
0137A	D412	Elongation at break	%	140
0159A	D624	Tear strength - die B	kN/m	2.6
0022	D0792	Specific gravity at 23°C		1.05
		Volume coefficient of thermal expansion	1/K	$9.6x10^{a}$
		Coefficient of thermal conductivity	W/(m.K)	0.17
		Electrical properties, cured 4 hours at 65°C		
0114	D149	Dielectric strength	kV/mm	21
0112	D150	Permittivity at 100Hz		2.75
0112	D150	Permittivity at 100kHz		2.75
0112	D150	Dissipation factor at 100Hz		0.001
0112	D150	Dissipation factor at 1kHz		0.001
0249	D257	Volume resistivity	Ohm.cm	$5x10^{l}$
		Comparative tracking index (IEC112)		600

1. Brookfield LVF, spindle #4 at 60rpm
2. Time required for catalysed viscosity to double at 23°C.

* CTM: Corporate Test Method, copies of CTMs are available on request.
ASTM: American Society for Testing and Materials.

HOW TO USE

Substrate preparation

All surfaces should be cleaned and degreased with a suitable solvent prior to potting. Care should be taken to ensure that all solvent is removed.

For best adhesion, coat surfaces with DOW CORNING® 92-023 Primer or DOW CORNING® 1200 OS Primer, following the instructions and precautions given for use of these products.

Mixing

SYLGARD 184 Silicone Elastomer is supplied in lot matched kits consisting of base and curing agent in separate containers.

The two components should be thoroughly mixed using a weight or volume ratio of 10:1.

The pot life is 2 hours for catalysed SYLGARD 184 Silicone Elastomer at room temperature.

Vacuum de-airing is recommended. A residual pressure of 10-20mm mercury applied for 30 minutes will sufficiently de-air the material.

Lowering the viscosity

The viscosity of SYLGARD 184 Silicone Elastomer may be reduced by addition of up to 10% of DOW CORNING® 200 Fluid 20 cS. Added quantities of less than 5% have little or no effect on either the physical or electrical properties while larger quantities of DOW CORNING 200 Fluid 20 cS will diminish the physical strength and hardness. The addition of DOW CORNING 200 Fluid 20 cS does not alter the amount of curing agent required.

How to apply

Apply the encapsulant, being careful to avoid air entrapment. Vacuum encapsulation is recommended for complex geometries.

For information on appropriate dispensing equipment for your application, please contact Dow Corning.

Curing

SYLGARD 184 Silicone Elastomer should be cured using one of the following recommended schedules:

24 hours at 23°C, or
4 hours at 65°C, or
1 hour at 100°C, or
15 minutes at 150°C

Large components and assemblies may require longer times in order to reach the curing temperature.

At 23°C the material will have cured sufficiently in 24 hours to be handled; however full mechanical and electrical properties will only be achieved after 7 days.

Compatibility

In some cases, SYLGARD 184 Silicone Elastomer may fail to cure to optimum properties when in contact with certain plastics or rubbers. Cleaning the substrate with solvent or baking slightly above the cure temperature will normally eliminate the problem.

Certain chemicals, curing agents and plasticisers can inhibit cure. These include:

- Organo-tin compounds
- Silicone rubber containing organo-tin catalysts
- Sulphur, polysulphides, polysulphones and other sulphur containing materials
- Amines, urethanes, amides and azides.

HANDLING PRECAUTIONS

PRODUCT SAFETY INFORMATION REQUIRED FOR SAFE USE IS NOT INCLUDED. BEFORE HANDLING, READ PRODUCT AND SAFETY DATA SHEETS AND CONTAINER LABELS FOR SAFE USE, PHYSICAL AND HEALTH HAZARD INFORMATION. THE SAFETY DATA SHEET IS AVAILABLE FROM YOUR LOCAL DOW CORNING SALES REPRESENTATIVE.

USABLE LIFE AND STORAGE

When stored at or below 32°C in the original unopened containers, this product has a usable life of 24 months from the date of production.

PACKAGING

SYLGARD 184 Silicone Elastomer is available in standard industrial container sizes. For details please refer to your Dow Corning sales office.

LIMITATIONS

This product is neither tested nor represented as suitable for medical or pharmaceutical uses.

HEALTH AND ENVIRONMENTAL INFORMATION

To support customers in their product safety needs, Dow Corning has an extensive Product Stewardship organization and a team of Health, Environment and Regulatory Affairs specialists available in each area.

For further information, please consult your local Dow Corning representative.

WARRANTY INFORMATION - PLEASE READ CAREFULLY

The information contained herein is offered in good faith and is believed to be accurate. However, because conditions and methods of use of our products are beyond our control, this information should not be used in substitution for customer's tests to ensure that Dow Corning's products are safe, effective, and fully satisfactory for the intended end use. Dow Corning's sole warranty is that the product will meet the Dow Corning sales specifications in effect at the time of shipment. Your exclusive remedy for breach of such warranty is limited to refund of purchase price or replacement of any product shown to be other than as warranted. Dow Corning specifically disclaims any other express or implied warranty of fitness for a particular purpose or merchantability. Unless

Dow Corning provides you with a specific, duly signed endorsement of fitness for use, Dow Corning disclaims liability for any incidental or consequential damages. Suggestions of use shall not be taken as inducements to infringe any patent.

® DOW CORNING and SYLGARD are registered trademarks of Dow Corning Corporation.
©1997-2001 Dow Corning Corporation. All rights reserved.

Revised: 02–June–2004

Working With FluoSpheres® Fluorescent Microspheres

Properties and Modifications

Introduction

Molecular Probes' FluoSpheres® microspheres are manufactured using high-quality, ultraclean polystyrene microspheres. These microspheres are loaded with Molecular Probes' proprietary dyes, making them the brightest fluorescent microspheres available. With our special staining methods, all of the fluorescent dye molecules are contained inside each polystyrene microsphere, instead of merely on the bead's surface. The protective environment within the bead shields the dye from many of the environmental effects that cause quenching or photobleaching of exposed fluorophores. The method we employ also ensures the narrow distribution of fluorescence intensity and size. The stability, uniformity and reproducibility of the FluoSpheres microspheres, as well as the extensive selection of colors available, make them the preferred tools for research and diagnostic assays that use fluorescence. In addition, fluorescent microspheres are potentially more sensitive than colorimetric methods in most, if not all, of the major microsphere-based diagnostic test systems presently in use, including microsphere-agglutination tests, filter-separation tests, particle-capture ELISA methods and two-particle sandwich techniques. Every possible precaution is made throughout the manufacturing process to ensure that the microparticles are kept free of contaminating agents. The final product is sold as a suspension in ultrapure water, in most cases containing 2 mM azide or 0.02% thimerosal as a preservative.

Surface Properties

FluoSpheres are available with four different surface functional groups, making them compatible with a variety of conjugation strategies. Our fluorescent dyes have a negligible effect on the surface properties of the polystyrene beads or on their protein adsorption. Anionic FluoSpheres having aldehyde–sulfate, sulfate or carboxylate-modified surface groups have been used most frequently in biological applications due to their broader general availability and because they are less likely to bind to negatively charged cell surfaces. Cationic microspheres having amine-modified surface groups have been used less frequently, but may have some distinct advantages for certain applications, since they are stable to alkaline pH conditions and to high concentrations of multivalent anions such as calcium and magnesium. We caution, however, that the surface properties have an important role in the functional utility of the microspheres; we cannot guarantee the suitability of a particular bead type for all applications.

Carboxylate-Modified FluoSpheres

The carboxylate-modified microsphere products are made by grafting polymers containing carboxylic acid groups to sulfate microspheres. The result is a microsphere with a highly charged, relatively hydrophilic and somewhat porous surface layer. The external layer produced by this modification process is only a few Å thick, and therefore does not change the size of the seed particles significantly. The surface charges of carboxylate-modified microspheres range between 0.1 and 2.0 milliequivalents/gram, and therefore, they are stable to relatively high concentrations of electrolytes (up to 1 M univalent salt). Carboxylate-modified microspheres will adsorb proteins and other biomolecules, but much less strongly than the hydrophobic microspheres. Carboxylate-modified microphores are often superior for applications in biological systems because they are more highly charged, which reduces their attraction to cells. It is also easier to further reduce nonspecific binding by the introduction of additives such as bovine serum albumin (BSA) or dextrans. A further potential advantage of carboxylate-modified microphores is that they can be covalently coupled to proteins, nucleic acids and other biomolecules. Covalent coupling requires more effort than passive adsorption, but can result in conjugates with greater specific activity and products that remain active longer. Covalent coupling to carboxylate-modified microspheres is the method of choice for conjugating low molecular weight peptides and oligonucleotides. Carbodiimide-mediated coupling of proteins to carboxylate-modified microspheres is discussed in more detail below in *Covalent Coupling of Proteins to Carboxylate-Modified Microspheres*. Their pendent carboxyl groups also make these microspheres suitable for covalent coupling of amine-containing biomolecules using water-soluble carbodiimide reagents such as EDAC.

Amine-Modified FluoSpheres

Amine-modified microsphere products are prepared by further chemical modification of carboxylate-modified microspheres to give hydrophilic particles with positively charged amine groups. The charge density is high, permitting their use in high ionic strength buffers. Amine-modified microspheres contain aliphatic amine surface groups that can be coupled to a wide variety of amine-reactive molecules, including succinimidyl esters and isothiocyanates of haptens and drugs or carboxylic acids of proteins, using a water-soluble carbodiimide. The amine surface groups can also be reacted with SPDP (S1531) to yield (after reduction) microspheres with sulfhydryl groups.

Sulfate and Aldehyde-Sulfate FluoSpheres

The FluoSpheres having sulfate surface groups are relatively hydrophobic particles that will passively adsorb almost any protein, including BSA, IgG and avidin or streptavidin. The aldehyde-sulfate microspheres are sulfate microspheres modified by the addition of surface aldehyde groups. These microspheres are designed to react with proteins and other amines under very mild conditions. The microsphere suspensions are stable at up to about 0.2 M univalent electrolyte concentrations, but will readily agglomerate in the presence of low concentrations of divalent cations unless stabilized by a hydrophilic coating. Sulfate microspheres (pK_a <2) are stable at acidic pH above their approximate pK_a. Even though they have charged surfaces, the hydrophobic microspheres will bind strongly to any molecule that has hydrophobic character, including proteins, nucleic acids and many small biomolecules such as drugs and hormones. The hydrophobic microsphere products are usually suitable for applications in systems that are free of biologicals and need no further modifications. In biological systems, including immunoassay applications, the microspheres can be easily coated with various proteins or polysaccharides that will greatly reduce their capacity to adsorb biomolecules nonspecifically. Specific, stable adsorption of proteins such as avidin, streptavidin and antibodies is accomplished simply by mixing the microspheres and the protein together and then separating the microsphere-bound protein from the unbound protein. Refer below to *Passive Adsorption of Proteins to Hydrophobic Microspheres* for details.

Optimization of Buffers

The type and density of the surface charges on the microspheres will dictate the best choice of buffer systems for their use in experiments. As a general rule, cationic buffers such as Tris should be avoided when using anionic microspheres (aldehyde–sulfate, sulfate, carboxylate-modified); conversely, borate, citrate or phosphate buffers should be avoided when using cationic microspheres (amine-modified). The ionic strength of the buffer should be kept as low as possible, especially when the microspheres are very small or have a low charge density. Since anionic microspheres are very sensitive to low concentrations of multivalent cations, calcium and magnesium salts should be avoided if at all possible. Cationic microspheres are not sensitive to these ions and may be best for applications in which high concentrations of these ions are anticipated. Because of their hydrophobic character, microsphere particles are great scavengers, therefore, the water used for preparation of buffers should be as pure as possible. Either doubly distilled water or high-purity ion-exchanged water is strongly recommended. In general, the smaller the particle size, the more critical are these requirements, since very small microspheres have fewer charge groups for stabilization. The pH of the buffer can be important when using carboxylate-modified or amine-modified microspheres. The carboxylate-modified microspheres should be used at a pH greater than about 5.0, while the amine-modified microspheres require a pH of less than about 9.0. If these conditions are not followed, the charge groups on these particles may be neutralized, leading to agglomeration. If agglomeration does occur as a result of incorrect pH, the particles can usually be redispersed by adjusting the pH to the correct range followed by gentle sonication.

Controlling Nonspecific Binding of Microspheres

Nonspecific binding is probably the most common problem that is encountered in working with microspheres and is often the major reason for abandoning an otherwise well-conceived experiment with microsphere particles. As mentioned above, the particles are generally hydrophobic, and although various modifications tend to make them less hydrophobic, it must be realized that the particles are polystyrene-based and therefore always retain some hydrophobic characteristics. In biological systems, most of the nonspecific binding problems are a result of hydrophobic interactions; however, some of the problems may also be caused by charge-based interactions (for example, a positively charged molecule attracted to a negatively charged microsphere surface). The best way to minimize these nonspecific binding events is to coat the microsphere with a large macromolecule such as a protein or a polysaccharide, which reduces nonspecific binding by blocking the hydrophobic or charged binding sites on the microsphere surface. Although many types of coating agents may be used, the most frequently employed are bovine serum albumin (BSA), egg albumin and whole serum. Egg albumin should be avoided in systems that employ biotin–avidin binding. When using the hydrophobic microspheres, all that is usually necessary is to suspend the particles in a 1% solution of the protein-based coating agent, since at this concentration, the particles will be completely and stably coated.

Dextrans can be used as coating agents in place of or in addition to proteins. Unlike proteins, the hydrophilic dextrans bind reversibly to microspheres. They form a layer at the surface of the particles and make them more hydrophilic, thus reducing nonspecific interactions. If dextrans are used as coating agents, 40,000 MW dextran at a 2% weight/volume ratio is recommended. If the particle is a hydrophilic carboxylate-modified microsphere, the coating agent may not bind strongly enough to the particles and may fail to prevent nonspecific binding. In this case, covalent coupling of a coating agent such as BSA may solve the problem. In this method, specific binding proteins, such as immunoglobulin or avidin, can be mixed with BSA and simultaneously coupled covalently, resulting in a specifically active microsphere with a covalently bound BSA coating. As a last resort, or in situations where the use of detergents is acceptable, nonionic surfactants such as polyoxyethylenes (Triton® X-100 or Tween® 80) can be coated onto the microsphere at concentrations ranging from 0.01–0.1% (the exact amount to be determined by experimentation).

Our BlockAid™ blocking solution (B10710), a protein-based blocking solution, is designed for use with our streptavidin-, NeutrAvidin-, biotin- and protein A–labeled FluoSpheres microspheres. In flow cytometry applications, we find BlockAid blocking solution to be superior to other commercially available blocking solutions and to a number of “home-made” blocking solutions described in the scientific literature. We expect BlockAid blocking solution to be useful for preventing the nonspecific binding of protein-coated or other macromolecule-coated microspheres in a variety of flow cytometry and microscopy applications. BlockAid blocking solution is available in a 50-mL unit size.

Keeping FluoSpheres in a Monodisperse State

Microsphere particles, which are hydrophobic by nature, will always tend to agglomerate. In aqueous suspensions, the only thing preventing this is the surface charge on the particles. Surfactant-free microspheres do not have detergents to aid in dispersion, so these preparations are slightly more sensitive to conditions that can lead to agglomeration. These conditions include: 1) high concentration of particles; 2) high electrolyte concentration; and 3) neutralization of surface charge groups. To minimize these adverse conditions, it is always wise to keep the microsphere suspensions dilute. Recommended particle concentrations to be used when coating microsphere particles with proteins (both passive adsorption and covalent coupling) is 0.5–1.0% solids. Reaction buffers and storage buffers of relatively low ionic strength (100 mM or less) are best. The use of multivalent cations should be especially avoided with anionic microsphere particles. Finally the pH should be maintained so that all of the surface charges on the microsphere particles are fully ionized. If agglomeration does occur, the particles can frequently be rescued by either diluting the microsphere suspension, adjusting the pH or reducing the ionic strength and then redispersing the suspension by means of a bath sonicator. The use of a bath sonicator greatly aids in working with microsphere suspensions, and it is strongly recommended that this device be utilized if possible. Routine sonication of microsphere preparations is advised before each use, especially in critical applications where a high degree of monodispersity is required. In the case of very small particles (less than 0.1 µm), the sonicated suspension can be briefly centrifuged at high speed (12,000 rpm) to further remove agglomerates from the suspension (the monodisperse particles will remain in suspension under these conditions).

Passive Adsorption of Proteins to Hydrophobic Microspheres

Passive adsorption of proteins and other molecules having hydrophobic domains to microspheres is the simplest method of coating, since no chemical reactions are necessary. The coated microsphere product can often be purified from unbound ligand by a simple centrifugation and washing procedure. Passive adsorption should be used only with the hydrophobic microspheres (sulfate surface groups). The hydrophobic interactions that bind macromolecules to the microsphere particles are essentially independent of pH; however, pH and charge can influence the conformation of protein molecules and thus facilitate their binding. Virtually every protein studied to date has been shown to bind to hydrophobic microspheres, and, in general, proteins have been shown to bind most efficiently at a pH that is near their isoelectric point.

The microsphere particle concentration most suitable for adsorption is in the range of 0.5–1% solids. At this relatively low concentration of particles, the aggregation caused by protein bridging is minimized. The ligand to be attached should be added to the dilute suspension of microsphere particles at a concentration of 20–50 µg/mL of final suspension in a buffer with an ionic strength of less than 100 mM. The suspension is stirred, shaken or rocked gently for a period of a few minutes to a day or more at room temperature. While the physical adsorption is very fast and is complete in just a few seconds, protein-dependent conformational changes can take an hour or two for completion. It should be noted that partial coverage of the microsphere particles with a ligand usually produces a system with greater binding specificity than one where full surface coverage is achieved.

In order to avoid nonspecific adsorption of further proteins when the coated microsphere is used in applications such as a diagnostic test, the microsphere can be back-coated with albumin, gelatin or other macromolecules (0.5–1 mg/mL). These substances will fill in any remaining hydrophobic areas on the particles. If the application of the coated microsphere particles is such that detergents can be tolerated, a nonionic surfactant such as Tween 20 or Triton X-100 can be added to increase hydrophilicity of the particles.

The coated microsphere particles can be separated from unbound ligand by centrifugation and washing if the particle diameter is greater than about 0.2 µm. The smaller the particles, the greater the centrifugation force and time that will be required to cause them to sediment. Some care should be taken to avoid excessive centrifugation force, however; otherwise, the particles may be packed together too tightly and will overcome the repulsive forces between the particles. After the supernatant is carefully removed, the particles are resuspended in washing buffer by vortexing or sonication. In the case of microsphere particles with diameters of less than about 0.2 µm, some type of filtration process will be necessary for separation of unbound ligand. If the ligand is small, ordinary dialysis tubing (12,000–14,000 MW cut-off) can be used; otherwise, cellulose ester dialysis tubing with a MW cut-off of 300,000 daltons can be used for most proteins, including IgG. When dialyzing the particles, the buffer should be the same as that used for the adsorption process, and at least five changes of buffer should be made. Other separation processes such as gel filtration can also be used, although in our experience, the microsphere particles tend to stick nonspecifically to some types of gels.

Covalent Coupling of Proteins to Carboxylate-Modified Microspheres

There are many procedures published in the literature that describe covalent coupling of proteins and other macromolecules to carboxylate-modified microspheres. Almost all of these use a water-soluble carbodiimide (EDAC) to activate the surface carboxyl groups on the microsphere particles. The following procedure is a simple one-step method we have used with excellent results in our laboratory for coupling avidin, streptavidin, BSA and goat anti-mouse to our carboxylate-modified FluoSphere microspheres. The reaction can be easily scaled up or down to fit individual needs.

1.1 Prepare 100 mL of 50 mM phosphate buffer, pH 7.4, containing 0.9% NaCl (50 mM PBS).

1.2 Prepare 100 mL of 50 mM MES buffer, pH 6.0.

1.3 Dissolve 10–25 mg of protein (avidin, streptavidin, IgG, BSA, etc.) at 2–5 mg/mL in MES buffer in a glass centrifuge tube.

1.4 Add 5 mL of a 2% aqueous suspension of carboxylate-modified microsphere (note **A**). Incubate at room temperature for 15 minutes.

1.5 Add 40 mg of EDAC (1-ethyl-3-(3-dimethylaminopropyl)-carbodiimide; Molecular Probes' E2247). Mix by vortexing (note **A**).

1.6 Adjust the pH to 6.5 ± 0.2 with dilute NaOH. Incubate the reaction mixture on a rocker or orbital shaker for 2 hours at room temperature (or overnight, if desired) (note **A**).

1.7 Add glycine to give a final concentration of 100 mM to quench the reaction. Incubate 30 minutes at room temperature.

1.8 Centrifuge to separate the protein-labeled microsphere particles from unreacted protein. The time and speed of the centrifugation will vary with the diameter of the microsphere particles. As a guideline, 0.5 µm particles and smaller should be centrifuged at 25,000 × g for 30–60 minutes. Particles 1.0 µm and greater can usually be sedimented at 3000–5000 × g for 20 minutes. It may not be possible to centrifuge 20 nm and 40 nm particles without extended spin times. We therefore recommend that dialysis be used with beads of this size (note **B**).

1.9 Resuspend the pellet in 50 mM PBS by gentle vortexing or by use of a bath sonicator. Centrifuge as described in step 1.8.

1.10 Repeat step 1.9 twice more (a total of 3 washes).

1.11 Resuspend the protein-conjugated microspheres in 5 mL of 50 mM PBS. Other buffers compatible with the microspheres (see above) are also suitable. If desired, the microspheres can be resuspended in a final buffer containing 1% BSA. The BSA will adsorb to the remaining hydrophobic sites on the microspheres and help to provide a more stable suspension that may be less prone to nonspecific interactions with other proteins.

1.12 Add 2 mM sodium azide and store the microspheres at 4°C. DO NOT FREEZE.

Covalent Coupling of Proteins to Aldehyde–Sulfate Microspheres

Aldehyde–sulfate FluoSpheres microspheres can be conjugated to proteins via the formation of a Schiff base between the aliphatic aldehyde surface groups and the lysine ϵ-amines of proteins. Coupling of proteins to aldehyde–sulfate microspheres is simpler than the method described above for carboxylate-modified microspheres, in that there is no need to use an activating reagent. The procedure given below is a one-step mix-and-wash protocol, resulting in a coated microsphere with covalently bound protein on the surface. As with the procedure for coupling proteins to carboxylate-modified microspheres (previous section), the reaction can be scaled to meet individual needs.

2.1 Prepare 100 mL of 50 mM phosphate buffer, pH 7.4, containing 0.9% NaCl (50 mM PBS).

2.2 Prepare 100 mL of 50 mM phosphate buffer, pH 6.5.

2.3 Dissolve 4 mg protein (avidin, streptavidin, IgG, BSA, etc.) in 2 mL phosphate buffer, pH 6.5, in a 15 mL glass centrifuge tube.

2.4 Add 5 mL of a 2% aqueous suspension of aldehyde–sulfate microspheres. Incubate at room temperature overnight.

2.5 *(optional)* The reaction of aldehyde groups with amines to form a Schiff base is a reversible reaction; however, since several different amine groups on a given protein molecule are coupled simultaneously to the microsphere particle, thermodynamics are unfavorable for dissociation of the protein from the microsphere surface. The Schiff base adduct can be reduced, if desired, to a stable alkylamine bond by addition of 15 mg of sodium cyanoborohydride immediately after addition of the microsphere suspension in step 2.4. Reduction of the Schiff base with cyanoborohydride is advised when small peptides or other molecules with only one reactive amine group are conjugated to aldehyde-sulfate microspheres.

2.6 Centrifuge to separate the protein-labeled microsphere particles from unreacted protein. See steps 1.8–1.11 for details for purification of the protein-coated microspheres.

Notes

[A] Agglomeration of the microsphere particles may be observed at this point in the procedure. This agglomeration can be caused by bridging of the particles by protein, neutralization of the charged carboxyl groups or both. Adjusting the pH to 6.5 and sonication of the mixture in a bath sonicator usually will redisperse the particles. If the particles do not redisperse with these treatments, try a lower concentration of particles and reagents (begin with a 50% reduction in concentration).

[B] Particles with a diameter <0.2 µm can be separated from unbound ligand by dialysis using 100,000–300,000 MW cut-off cellulose ester dialysis tubing (Spectrapor, Spectrum Medical Industries, Los Angeles). We have confirmed that this method effectively removes BSA, avidin and IgG from microsphere particles with average diameters ranging from 0.03 to 1.0 µm.

Contact Information

Further information on Molecular Probes' products, including product bibliographies, is available from your local distributor or directly from Molecular Probes. Customers in Europe, Africa and the Middle East should contact our office in Leiden, the Netherlands. All others should contact our Technical Assistance Department in Eugene, Oregon.

Please visit our Web site — **www.probes.com** — for the most up-to-date information

Molecular Probes, Inc.
29851 Willow Creek Road, Eugene, OR 97402
Phone: (541) 465-8300 ● Fax: (541) 335-0504

Customer Service: 6:00 am to 4:30 pm (Pacific Time)
Phone: (541) 335-0338 ● Fax: (541) 335-0305 ● order@probes.com

Toll-Free Ordering for USA and Canada:
Order Phone: (800) 438-2209 ● Order Fax: (800) 438-0228

Technical Assistance: 8:00 am to 4:00 pm (Pacific Time)
Phone: (541) 335-0353 ● Toll-Free: (800) 438-2209
Fax: (541) 335-0238 ● tech@probes.com

Molecular Probes Europe BV
Poortgebouw, Rijnsburgerweg 10
2333 AA Leiden, The Netherlands
Phone: +31-71-5233378 ● Fax: +31-71-5233419

Customer Service: 9:00 to 16:30 (Central European Time)
Phone: +31-71-5236850 ● Fax: +31-71-5233419
eurorder@probes.nl

Technical Assistance: 9:00 to 16:30 (Central European Time)
Phone: +31-71-5233431 ● Fax: +31-71-5241883
eurotech@probes.nl

Molecular Probes' products are high-quality reagents and materials intended for research purposes only. These products must be used by, or directly under the supervision of, a technically qualified individual experienced in handling potentially hazardous chemicals. Please read the Material Safety Data Sheet provided for each product; other regulatory considerations may apply.

Several of Molecular Probes' products and product applications are covered by U.S. and foreign patents and patents pending. Our products are not available for resale or other commercial uses without a specific agreement from Molecular Probes, Inc. We welcome inquiries about licensing the use of our dyes, trademarks or technologies. Please submit inquiries by e-mail to busdev@probes.com. All names containing the designation ® are registered with the U.S. Patent and Trademark Office.

Copyright 2004, Molecular Probes, Inc. All rights reserved. This information is subject to change without notice.

428-PROG

Programmable Current Amplifier

- **2µs rise time**
- **1.2fA rms noise**
- **Up to 10^{11} V/A gain**
- **IEEE-488 interface**

Ordering Information

428-PROG
Programmable Current Amplifier with IEEE-488 Interface

Extended warranty, service, and calibration contracts are available.

APPLICATIONS

The Model 428-PROG satisfies a broad range of applications in research and device labs due to its cost-effective ability to amplify fast, low currents. A few of these applications include:

Biochemistry Measurements:

- Ion channel currents through cell walls and membranes

Beam Position Monitoring:

- Used on electron storage rings and synchrotrons

Surface Science Studies:

- Scanning Tunneling Electron Microscope system amplifier
- Observation of secondary electron emission, as in X-ray and beam line currents

Laser and Light Measurements:

- Fast, sensitive amplifier for use with PMTs and photodiodes
- Analysis of fast photoconductive materials.
- IR detector amplifier

Transient Phenomena:

- Current DLTS studies
- Breakdown in devices and dielectric materials

The Model 428-PROG Programmable Current Amplifier converts fast, small currents to a voltage, which can be easily digitized or displayed by an oscilloscope, waveform analyzer, or data acquisition system. It uses a sophisticated "feedback current" circuit to achieve both fast rise times and sub-picoamp noise. The gain of the Model 428-PROG is adjustable in decade increments from 10^3V/A to 10^{11}V/A, with selectable rise times from 2µs to 300ms.

The Model 428-PROG offers fast response at low current levels, which is unmatched by either electrometers or picoammeters. The nine current amplification ranges allow the greatest flexibility in making speed/noise tradeoffs. The Model 428-PROG can be used with any of Keithley's data acquisition boards to implement a very cost-effective, low curreent measurement system with wide bandwidth and fast response.

The Model 428-PROG incorporates a second-order Bessel-function filter that minimizes noise without increasing rise time on high-gain ranges. This can be defeated in situations where 6dB/octave roll-off is desired, as in control loops of scanning tunneling electron microscopes.

Input and output connections to the Model 428-PROG are made with BNC connectors. INPUT HI is connected to a programmable ±5V supply, which permits suitable bias voltages to be applied to devices-under-test or current collectors. This eliminates the need for a separate bias supply.

For applications where voltage offset errors exist, the ZERO CHECK and OFFSET functions can be used, thereby maintaining maximum instrument accuracy. Current suppression is also available up to 5mA, useful for suppressing background currents, such as dark currents.

The Model 428-PROG also incorporates an exterior design with simple front panel operation, improved display, and convenient system integration. Pushbutton controls have an LED to indicate if that function is activated. The display features three selectable intensities (bright, dim, and off) for use in light-sensitive environments. All setup values can be displayed from the front panel. An IEEE-488 interface is included.

The Model 428-PROG as Preamplifier to an Oscilloscope

The Model 428-PROG can be connected to an oscilloscope or waveform digitizer to display very low currents in real time.

Converts small, fast currents to a voltage

LOW LEVEL MEASURE & SOURCE

1.888.KEITHLEY (U.S. only)
www.keithley.com

KEITHLEY

A GREATER MEASURE OF CONFIDENCE

428-PROG Programmable Current Amplifier

GAIN SETTING V/A	ACCURACY[1] 18°–28°C ±(% input + offset)	ACCURACY[1] TEMPERATURE COEFFICIENT ±(% input + offset)/°C	LOW NOISE[2] RISE TIME[3] (10%–90%) ms	LOW NOISE[2] NOISE rms	MAXIMUM SPEED RISE TIME[3] (10%–90%) µs[4]	MAXIMUM SPEED NOISE rms[4]	DC INPUT RESISTANCE
10^3	0.45 + 1.2 µA	0.01 + 40 nA	0.1	90 nA	2	100 nA	< 0.6Ω
10^4	0.31 + 120 nA	0.01 + 4 nA	0.1	9 nA	2	15 nA	< 0.7Ω
10^5	0.31 + 12 nA	0.01 + 400 pA	0.1	900 pA	5	2 nA	< 1.6Ω
10^6	0.34 + 1.2 nA	0.01 + 40 pA	0.1	90 pA	10	500 pA	< 10 Ω
10^7	0.5 + 122 pA	0.015 + 4.3 pA	0.1	9 pA	15	200 pA	< 100 Ω
10^8	1.4 + 14 pA	0.015 + 700 fA	1	0.5 pA	40	30 pA	< 1kΩ
10^9	2.5 + 3 pA	0.025 + 300 fA	10	50 fA	100	10 pA	< 10kΩ
10^{10}	2.5 + 1.6 pA	0.025 + 250 fA	100	4 fA	250	2 pA	< 100kΩ
10^{11}*	2.7 + 1.6 pA	0.028 + 250 fA	300	1.2 fA	250	2 pA	< 100kΩ

[1] When properly zeroed using zero correct.
[2] Selectable filtering will improve noise specifications; see operator's manual for details (typical value shown).
[3] Bandwidth = 0.35/rise time.
[4] With up to 100pF shunt capacitance; autofilter on; low pass filter off.
* 10^{11} setting is 10^{10} setting with GAIN ×10 enabled; other entries are for GAIN ×10 disabled.

SPECIFICATIONS

INPUT:

Voltage Burden: <200µV (18°–28°C) for inputs <100µA; <10mV for inputs ≥ 100µA; 20µV/°C temperature coefficient.

Maximum Overload: 100V on 10^4 to 10^{11}V/A ranges; 10V on 10^3V/A range. Higher voltage sources must be current limited at 10mA.

OUTPUT:

Range: ±10V, 1mA; bias voltage off.

Impedance: <100Ω DC–175kHz.

LOW PASS FILTER:

Ranges: 10µs to 300ms (±25%) in 1, 3, 10 sequence or OFF.

Attenuation: 12dB/octave.

GAIN ×10: Rise time, noise, and input resistance are unchanged when selecting GAIN ×10; gain accuracy and temperature coefficient are degraded by 0.2% and 0.003%/°C respectively.

CURRENT SUPPRESSION

RANGE	RESOLUTION	ACCURACY ±(%setting + offset)
±5 nA	1 pA	3.0 + 10 pA
±50 nA	10 pA	1.6 + 100 pA
±500 nA	100 pA	0.8 + 1 nA
±5 µA	1 nA	0.7 + 10 nA
±50 µA	10 nA	0.6 + 100 nA
±500 µA	100 nA	0.6 + 1 µA
±5 mA	1 µA	0.6 + 10 µA

BIAS VOLTAGE:

Range: ±5V

Resolution: 2.5mV

Accuracy: ±(1.1%rdg + 25mV).

Model 428-PROG rear panel

GENERAL

DISPLAY: Ten character alphanumeric LED display with normal/dim/off intensity control.

REAR PANEL CONNECTORS:

Input BNC: Common connected to chassis through 1kΩ.

Output BNC: Common connected to chassis.

IEEE-488 Connector

5-Way Binding Post: Connected to chassis.

EMI/RFI: Complies with the RF interference limits of FCC Part 15 Class B and VDE 0871 Class B.

EMC: Conforms to European Union Directive 89/336/EEC.

SAFETY: Conforms to European Union Directive 73/23/EEC (meets EN61010-1/IEC 1010).

WARM-UP: 1 hour to rated accuracy.

ENVIRONMENT: Operating: 0°–50°C, <70% R.H. up to 35°C; linearly derate R.H. 3%/°C up to 50°C. Storage: –25°C to 65°C.

POWER: 105–125VAC or 210–250VAC, switch selected. (90–110/180–220VAC available.) 50Hz or 60Hz. 45VA maximum.

DIMENSIONS: 90mm high × 213mm wide × 397mm deep (3½ in × 8⅜ in × 15⅝ in).

IEEE-488 BUS IMPLEMENTATION

PROGRAMMABLE PARAMETERS: All parameters and controls programmable except for IEEE-488 bus address.

EXECUTION SPEED: (measured from DAV true to RFD true on bus).
Zero Correct & Auto Suppression commands: <3s.
Save/Recall Configuration commands: <500ms.
All other commands: <40ms.

ACCESSORIES AVAILABLE

CABLES

4801	Low Noise BNC Input Cable, 1.2m (4 ft)
7007-1	Shielded IEEE-488 Cable, 1m (3.3 ft)
7007-2	Shielded IEEE-488 Cable, 2m (6.6 ft)

ADAPTERS

7078-TRX-BNC	3-Slot Male Triax to Female BNC Adapter
KPCI-488LP	IEEE-488 Interface/Controller for the PCI Bus
KPXI-488	IEEE-488 Interface Board for the PXI Bus
KUSB-488A	IEEE-488 USB-to-GPIB Interface Adapter (requires 7010 Adapter)

RACK MOUNTS

4288-1	Single Fixed Rack Mount Kit
4288-2	Dual Fixed Rack Mount Kit

1.888.KEITHLEY (U.S. only)
www.keithley.com